©2011 Society of Economic Geologists, Inc.
Economic Geology, v. 106, pp. 975–998

Structural Evolution of a World-Class Epithermal Orebody: The Martha Hill Deposit, Waihi, New Zealand

K. Bernard Spörli[1,†] and Hugh Cargill[2]

[1] *Geology Programme, School of Environment, University of Auckland, Private Bag 92019, Auckland 1142, New Zealand*

[2] *28 Norwich Avenue, New Plymouth 4310, New Zealand*

Abstract

We describe the complex structure in the highest (now mined-out) levels of the world-class Martha Hill gold-silver deposit, Coromandel peninsula, which is hosted in late Miocene andesitic rocks. A northeast-striking block of rock 360 m long and up to 100 m wide was occupied by a complex vein network dominated by northeast-striking gold-silver lodes up to 30 m thick. Gold production was entirely from quartz veins. The mineralization is embedded in the following geological history: (1) deposition of the host volcanic rocks, (2) initial tectonic fracturing, (3) intrusion of clastic dikes and sills, (4) start of hydrothermal alteration, (5) main phase of faulting, (6) main phase of veining, (7) erosion and deep oxidation, (8–11) deposition of further volcanic material, including prominent rhyolites, and formation of present topography. Veins occupied fractures but also followed a network of preexisting, mostly normal faults with a small to medium amount of displacement. Faulting involved northwest-southeast, north-south, and east-west extension, implying complex 3-D strain. Clastic dikes of carbonaceous sandstone intruded during the faulting phase. Fault rocks were mostly brittle cataclasites or breccias, but some clay-rich zones displayed ductile structures. Many veins overprinted faults, with a change from shear-mode to opening-mode deformation. Stockwork veins formed a mesh composed of two orthogonal sets: one with northeast-southwest– and northwest-southeast–striking veins, including the dominant mineralized lodes, and the other with north-south– and east-west–striking veins. Although northwest-striking veins were earliest, during the main vein phase, opening oscillated between all the vein directions, with the two main lodes in the open pit area, the Martha and the Welcome, capturing most of the strain. A variety of vein and breccia textures indicate repeated structurally controlled vein opening events that were associated with changes in the physical and chemical conditions of the mineralizing fluid. A special concentration of structural features facilitated focusing of fluid flow to produce this world-class deposit, which contrasts with the less well endowed vein systems around it. The overall tectonic control was dominated by northwest-southeast extension and dip-slip deformation. The 3-D strain in this area was not only due to local interference of differently oriented structural features but also to the superposition of regional tectonic north-northwest and northeast trends associated with migration of a subduction zone past the Coromandel peninsula. This demonstrates that structural control in an epithermal mineral deposit may originate from a number of different tectonic controls at different scales.

Introduction

Epithermal deposits record deformation at the shallowest levels in the crust, where inhomogeneity, low confining pressures and, in some cases, the configuration of the Earth's surface can provide additional complexity. Although the general setting of epithermal deposits has been well described (Simmons et al., 2005, and references therein), the actual structural controls of vein formation and of mineral deposition have received less attention (e.g., Berger et al., 2003; Chauvet et al., 2006; Micklethwaite, 2009) and are often approached from a theoretical rather than an observational point of view (e.g., Sibson, 1987, 1996). Therefore, a structural study of a major, superbly exposed epithermal gold deposit can provide much needed observational ground truth for the processes that may operate in this environment. The world-class Martha Hill mine in the Hauraki goldfield of New Zealand (Figs. 1, 2), with a total mined and unmined resource of greater than 7 Moz Au, provides such an opportunity.

This paper describes the state of structural information in the Martha Hill mine up to 1994, as presented by Cargill (1994), and therefore treats only the upper levels of the total vein system (Figs. 3–5). Future work may allow recognition of downward changes in structural style towards the now-exposed deeper levels of the mine similar to the downward disappearance of microcrystalline quartz and adularia (Brathwaite and Faure, 2002; Brathwaite et al., 2006; Martin and Mauk, 2006). We first describe the relevant structures, with special attention to faults and vein patterns and the relationship between the two. Vein textures are also considered because they help constrain fluid flow and vein opening events. We then discuss the significance of all these features to the detailed structural history and control of the vein system, as well as to the tectonics of the Coromandel peninsula. Finally, comparisons are made with some of the other epithermal gold deposits in the Hauraki goldfield and overseas.

[†] Corresponding author: e-mail, kb.sporli@auckland.ac.nz

Regional and Local Geology

The Martha Hill mine is part of the Hauraki goldfield on the Coromandel peninsula of northern New Zealand (Christie et al., 2007) (Fig. 1). The goldfield comprises about 50 mineral deposits hosted in late Miocene to early Pleistocene arc/back-arc volcanic rocks of the Coromandel volcanic zone of Skinner (1986). These volcanic rocks are subdivided into the older Coromandel Group andesites (early Miocene-early Pliocene) and the younger Whitianga Group rhyolites (late Miocene-late Pliocene). The rhyolites are associated with a

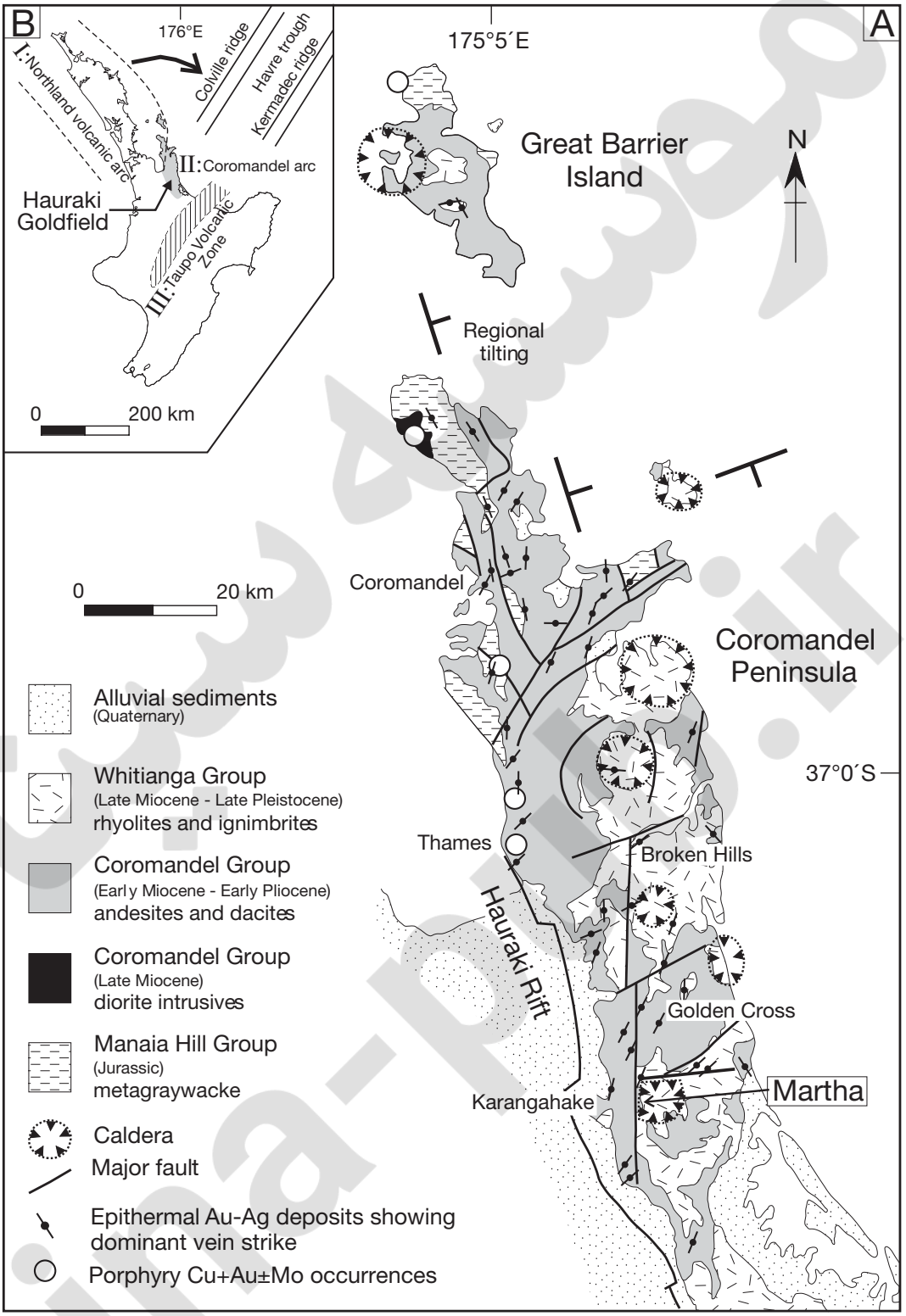

FIG. 1. Geological setting of the Hauraki goldfield on the Coromandel peninsula and location of the Martha Hill mine, modified after Skinner (1986), Brathwaite et al. (1989), Simpson and Mauk (2007). (A) Main map. Note the exposure of Mesozoic basement rocks (Manaia Hill Group), interference of post-Miocene eastward and southward tilting (large strike and dip symbols) in the north, and the caldera structures associated with the Whitianga Group rhyolites. Northeasterly strikes of epithermal Au-Ag vein systems are most common in the southern half of the peninsula. (B) Position of Coromandel peninsula in the North Island of New Zealand and its relationship to offshore tectonic features, showing migration (curved arrow) of subduction zone and associated volcanic arcs from the northern end of the North Island to its present site (curved arrow). I: Late Oligocene-Miocene, II: Late Miocene-Pliocene, III: Pleistocene to present.

north-northwest–striking belt of calderas (Fig. 1A). Regional basement consists of Mesozoic low-grade metagraywackes (Manaia Hill Group) unconformably capped by a thin sequence of Paleocene to Miocene coal measures, carbonates, mudstones and sandstones (Skinner, 1976; Dix and Nelson, 2004). These basement rocks rise up to 800 m a.s.l. at the north end of the Coromandel peninsula but descend to below sea level toward the south and southeast. Post-Miocene eastward and southward tilting (Fig.1A) influences the block fault-controlled map pattern of units in the northern part of the peninsula (Spörli et al., 2006). Northeast–, north-northwest–, and some north-south–striking faults, with large normal components of movement, are prominent throughout the peninsula (Fig.1A). The north-northwest–striking faults form a horst and graben pattern, whereas the northeasterly striking faults are predominantly downthrown to the south (Skinner, 1986). As in other areas of New Zealand (Spörli, 1987; King, 2000), it is likely that many of these have been inherited from a network of block-bounding basement faults formed during Cretaceous to early Tertiary rifting, and therefore may have been reactivated one or several times. However, there is little reliable information on the slip history of any of the faults on the Coromandel peninsula, mainly due to a dearth of suitable outcrops.

The western boundary of the Hauraki goldfield is formed by the north-south–striking Hauraki rift (Fig. 1A), which is the major active tectonic feature of the region (Hochstein and Ballance, 1993) and, depending on its age of inception, may have had significant tectonic influence on the development of the Hauraki goldfield. It is an asymmetric graben 25 to 45 km wide that can be traced for at least 250 km along strike. Displacement of the floor ranges up to 2.5 km. A central tilted horst coincides with an active fault and hot springs. Hochstein and Ballance (1993) suggest that rifting began 10 to 7 Ma ago (late Miocene); however, on the basis of the paleogeography of Oligocene carbonates, Dix and Nelson (2004) argue for an inception about 30 m.y. ago. On the other hand, three- to five-million-year-old gravels with vein quartz from the Hauraki goldfield occur on the western side of the Hauraki rift, which supports a post-Miocene inception (Hayward et al., 2006).

The basement rocks and their thin early Tertiary cover record Mesozoic accretionary tectonics on the margin of Gondwana up to the Early Cretaceous, followed by uplift, erosion, and subsidence during rifting of the New Zealand continental fragment away from the supercontinent (Spörli, 1987; King, 2000; Adams and Maas, 2004). In the late Oligocene, a new convergent plate boundary propagated southward through the North Island, leading to initial establishment of a volcanic arc in Northland by the Miocene. The subduction zone and its associated arc continued to migrate southward to its present position in the Taupo Volcanic Zone in central North Island (Fig. 1B). The Coromandel arc formed during the late Miocene to Pliocene stage of the migration (e.g., Hayward et al., 2001).

Interpretations of the Cenozoic tectonic history of the Coromandel volcanic arc are varied, but all are complex. The simplest scenario is a continuous migration of a single arc from Northland to the Taupo Volcanic Zone, as implied by the plate reconstructions of King (2000). Brathwaite and Skinner (1997) invoked collision of Northland with the Coromandel arc. They regarded the fault-controlled north-northwest strike of the Coromandel arc as due to a tectonic overprint on an arc extending southwest from the offshore Colville ridge (Fig. 1B). In this interpretation, the Colville arc and the Northland arc would both influence Coromandel volcanism. Spörli et al. (2006) attributed the differences in directions of vein strikes to interference of structures of the northeast-trending Havre trough-Colville ridge system offshore the Coromandel peninsula and the active Hauraki rift to the west (Fig. 1A). Mortimer et al. (2007, 2009) regarded Coromandel volcanism to be a direct continuation of the northeast-striking Colville arc. Mauk et al. (2011) propose that transfer of volcanism from the Northland arc to the Coromandel arc took place in the north part of the peninsula, accounting for a younging of the gold deposits to the south and a change from dominantly northwest-striking quartz veins in the north to northeast-striking veins in the south.

In the epithermal deposits of the Hauraki goldfield, gold is confined to quartz veins. A large proportion of gold production has been from northeast-striking veins (Christie et al., 2007). Christie et al. (2006) recognized a number of north-northeast–striking "structural corridors" with concentrated mineralization and alteration. One of these contains the Martha Hill mine. The Au-Ag deposits can be subdivided into three regional groups (Christie et al., 2007). In the northern group, many of the vein systems have north-south to north-northwest strikes and the vein fills are relatively simple. This is the only area where mineralization in the graywacke basement is exposed (Christie et al., 2007). Deposits in the eastern group, unlike those in the other groups, are mainly hosted in the Whitianga Group rhyolites, and some are clearly associated with caldera formation (Briggs and Krippner, 2006). Because of their greater permeability and lesser structural competence compared to the andesites of the underlying Coromandel Group, mineralized veins in the Whitianga Group are, on average, thinner, representing a smaller amount of extension by vein opening, but are more tightly clustered (Brathwaite et al., 2001). The Martha Hill mine (Figs. 1, 2) belongs to the southern group, which displays dominant north-northeast to northeast strikes of veins, more complex vein fills, and includes the largest gold producers in the field.

The epithermal Au-Ag deposits in the northern province have ages from 14.1 to 10 Ma and formed in an arc dominated by andesitic volcanism, whereas those in the eastern and southern deposits are associated with bimodal andesite-rhyolite volcanism, and their ages range from 7.1 to 5.7 Ma (Mauk and Hall, 2004; Mauk et al., 2011). The younger deposits account for eighty percent of the gold produced from the Hauraki goldfield.

The Martha Hill mine lies in the same block of altered rocks as the Union, Amaranth, Gladstone, and Favona deposits; together these deposits form the Waihi vein system (Torckler et al., 2006; Fig. 2). We note that individual veins strike northeast-southwest, but the Waihi vein system appears to form a west-northwest–east-southeast trend (Fig. 2). The Martha and Favona deposits are interpreted to represent two discrete upflow zones in one hydrothermal system (Simpson and Mauk, 2007). After its discovery in 1878, the Martha Lode vein array initially produced 217,000 kg of Au-Ag bullion

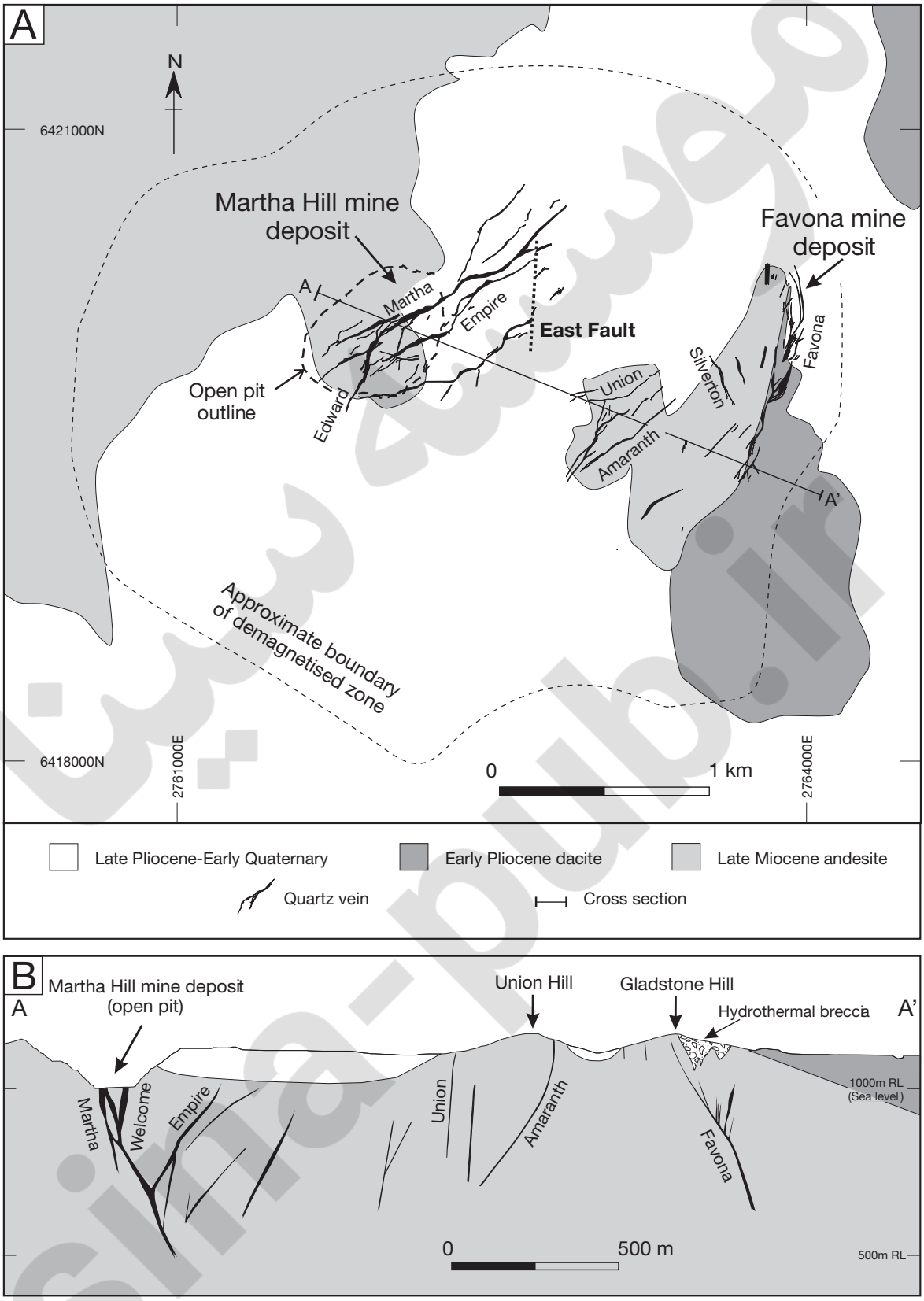

FIG. 2. (A) Geological map and location of the Martha Hill mine open pit (ellipse), after Simpson and Mauk (2007). Note the possible west-northwest–east-southeast alignment of the deposits versus the northeasterly trends of the main veins. The demagnetized zone defines the total Waihi up-flow system. (B) Cross section of the Waihi vein system.

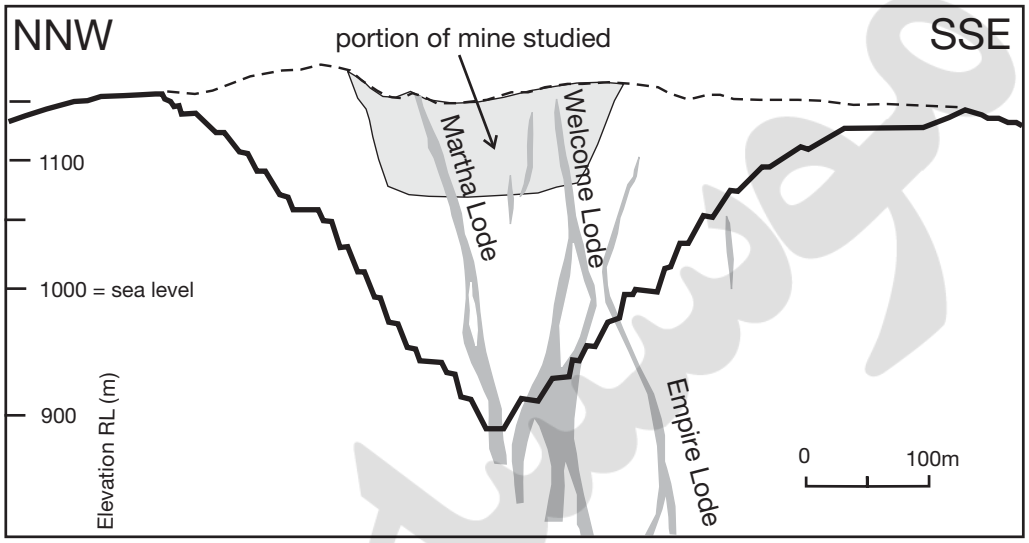

FIG. 3. Planned final section of the Martha Hill mine pit (with the major lodes shaded in darker gray) compared with the portion studied to 1994. Modified from Brathwaite et al. (2006). Note the overall steep south-south-eastward dip of main veined zone.

from underground workings along the major quartz veins until 1952. Since 1988, the Martha Hill mine has been worked as an open pit mine; total production from open pit and underground mining, through 2009, was 210,944 kg Au and 1,299,893 kg Ag (L. Torckler, writ. commun., 2010). Through 2006, the Martha Hill mine had produced 69 percent of the gold extracted from the Hauraki goldfield (Christie et al., 2007).

Host rocks of the vein system are the hydrothermally altered plagioclase-phyric two-pyroxene, locally quartz phenocryst-bearing andesites of the late Miocene Waipupu Formation (Brathwaite and Christie, 1996). The sequence includes some dacitic tuffs and thin carbonaceous lake beds dipping 40° SE (Brathwaite et al., 2006). Tuffs and tuff breccias are more abundant in the eastern part of the deposit. To the southeast of the Favona deposit, the Waipupu andesites are unconformably overlain by unaltered early Pliocene hornblende dacite of the Uretara Formation. However, in the Martha Hill mine area the host rocks are covered by a sequence of late Pliocene to Quaternary ignimbrites (Figs. 4, 5), which in the Waihi caldera basin to the south are underlain by carbonaceous lake sediments (Brathwaite and Christie, 1996; Smith et al., 2006). Regional faults are not exposed on the surface. Brathwaite et al. (2006) postulated a northeast-trending graben under the Waihi area (also see Hobbins, 2009).

In the Martha Hill mine, gold occurs in small grains (1–80 μm) of electrum (49.5–67.0 wt percent Au) with quartz or as inclusions in sulfides (Brathwaite and Faure, 2002). Initially, production was from the main lodes, but during the subsequent open pit stage it was also from the intervening stockwork of narrow veins. In the vein fills, there is a recurring sequence of initial platy calcite, quartz, pyrite and adularia, main stage quartz and sulfides ± electrum, and a final amethystine stage (Brathwaite and Faure, 2002). The ore is associated with crustiform banded quartz, some of which shows evidence of having been precipitated as colloids (Panther et al., 1995). In cross section, the vein system forms a steeply southeast-dipping band bounded by the major veins and internally dominated by smaller northward-dipping veins (Brathwaite et al., 2006, Fig. 5 of 7). The rocks have been affected by potassic, propylitic, and argillic alteration (Brathwaite and McKay, 1989). Based on $^{40}Ar/^{39}Ar$ plateau dates of adularia from a quartz vein, the preferred age for the Martha Hill mine deposit is 6.16 ± 0.06 Ma (Mauk et al., 2011). Fluid inclusion studies indicate main stage quartz deposition at 189° to 273° C with periodic boiling, and it is estimated that at least 160 m had been eroded off the top of the system prior to mining (Brathwaite and Faure, 2002). Over the total ~650 m mined, there is a downward transition from colloform quartz with electrum-bearing sulfides to crustiform quartz with electrum-poor sulfides (Brathwaite et al., 2006).

Methods and Sources of Data

Three sets of structural data are available from this stage of mining: (1) maps and structural measurements of veins on the pit floor at 1100 m RL, (2) strikes of veins, faults, and joints measured along benches, (3) logs of crosscutting structures.

For further understanding of the faulting, we used three methods to determine orientations of slip vectors on faults: (1) displacement of piercing points of the intersection line of two differently oriented offset markers (Fig. 6), (2) conjugate fault patterns and Riedel shears, and (3) striations (Fig. 7). While methods (1) and (2) provide both the slip vector and the sense of movement, for method (3) the sense of movement has to be independently deduced from the offset of, and/or drag on, a marker, from deflections in the fault geometry, or from mineral growth steps on the striated surface (Fig. 7C).

Traditionally, slip on faults has been directly related to the stress ellipsoid, where σ_1 is the largest principal stress axis, σ_2 the intermediate principal stress axis, and σ_3 the least principal stress axis (e.g., Anderson, 1951; Hancock, 1985). Although this simple link between deformation and stress may be reasonable for initial rupture of intact rock, or for incremental

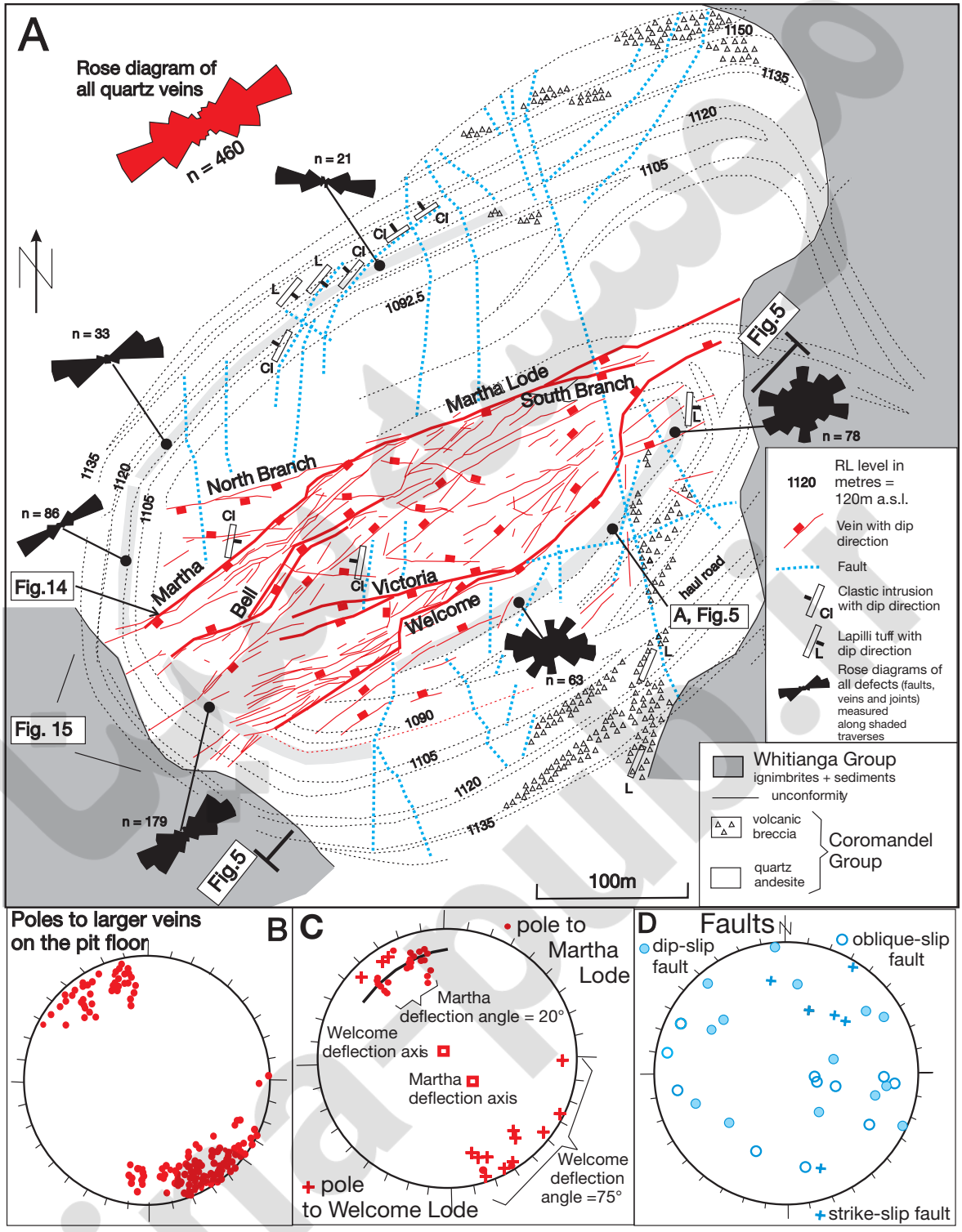

FIG. 4. (A) Map of the Martha Hill mine open pit of 1994. To simplify the figure, faults subparallel to the veins and within the vein array are not shown. Black rose diagrams are from traverse measurements of strikes of all defects (faults, veins, and joints) along portions of benches shaded light gray. Red rose diagram in upper left hand corner shows strikes of all quartz veins measured in the traverses. Numbers on benches indicate elevation (see legend in the figure for explanation). (B–C) Lower hemisphere equal area stereonet showing poles to planar structures. (B) Poles of the larger veins mapped on the pit floor, except those for Martha and Welcome lodes. (C) Orientation measurements along the Martha and Welcome lodes. Partial great circle patterns in their distribution (e.g., line through cluster of Martha lode vein poles) defines the deflection axis. The spread of poles along the great circle indicates the deflection angle. (D) Poles of faults on which slip vectors have been determined (Table 1). Note the predominance of dip-slip and oblique-slip movement and parallelism of some of the faults with vein orientations in (B) and (C).

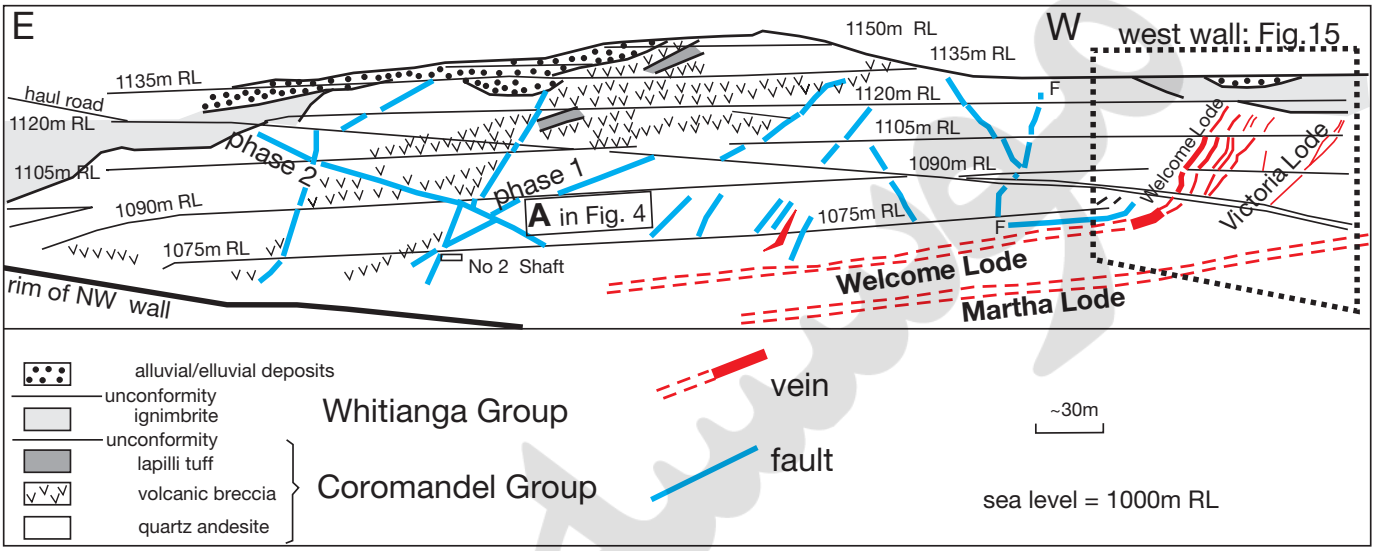

FIG. 5. View of the south wall of Martha Hill mine (location see Fig. 4A), showing the main lithological units, veins, and faults. Note fault parallel to Welcome lode. At A, an east-northeast–striking fault (phase 2) crosscuts two northerly striking faults (phase 1). Application of the piercing point method on the phase 2 fault (see text and Fig. 6), indicates 22 m of down-to-the-north displacement along a slip line pitching 83° to the east-northeast resulting from dominantly normal dip-slip with a very small component of dextral strike-slip.

movements (even during reactivation of faults), it is less appropriate for deducing the overall regime for an entire fault population active over a prolonged time span, where a terminology linked to the strain ellipsoid (extension, intermediate strain, contraction, or shortening) is more realistic (e.g., Wojtal, 2001; Townend and Zoback, 2005). We therefore restrict the use of the stress terminology for spot observations on individual fault planes, whereas regional fault patterns will be interpreted in terms of strain axes, despite the implied oversimplified assumption that stress axes have coincided with strain axes throughout deformation.

The orientation of σ_1, σ_2, and σ_3 can be modeled if both the orientation of the slip vector and the sense of movement on a fault are known (Fig. 7). In the case of conjugate faults and Riedel shears, the angle θ between σ_1 and the slip vector can be directly determined from the geometry (Figs. 7A, B), whereas for a single fault, a value of θ, usually 30°, based on empirical data from natural and experimental examples (e.g., Hancock, 1985), is assumed for modeling the orientation of the stress axes (Fig. 7C).

Stress axes can then be used to consider the compatibility of movement along variously oriented faults (e.g., Etchecopar et al., 1981; Angelier, 1984; Aleksandrowski, 1985). Stress axes from individual faults should have roughly similar orientations if they belong to the same system. This can also apply to groupings of normal, reverse, and strike-slip faults. However, in this case, some of the stress axes will be interchanged (Fig. 8). For instance, while strike-slip faults and reverse faults in such a system will have their largest principal stress axes in a common direction, the directions of their least and intermediate principal stress axes will be interchanged. Normal faults will have their least principal stress axes in the same direction as those of the strike-slip faults, but the directions of the other two axes will be interchanged (e.g., Wilcox et al., 1973; Harding, 1985; Sylvester, 1988). Such a fault array with interchanged stress axes indicates 3-D strain and is similar to the orthorhombic slip systems described by Krantz (1988).

The term "2-D (or plane) strain" indicates that the deformation is such that there have been changes in length only in the plane defined by two of the three axes of the strain ellipsoid, the axis of maximum strain and the axis of least strain, while the intermediate axis remains unchanged. Examples include a set of parallel extension veins, a simple en-echelon tension gash array, or a pair of conjugate faults. In "3-D (or nonplane) strain," the intermediate axis will also be involved, i.e., there can be changes in length in all directions within the rock mass being deformed (Krantz, 1988; Wojtal, 2001; Spörli et al., 2006). An example is a set of simultaneously opening multidirectional stockwork veins. The 3-D strain can lead to higher complexity and connectivity in a hydrothermal plumbing system.

Because most of the exposures that are the subject of this paper have been removed by mining, we use the past tense for our descriptions. Orientations of structural planes are given as strikes and dips in degrees, e.g., 135/20 SW, those of linear features as plunge and azimuth, e.g., 65/055. The specimens mentioned in the text are lodged in the geology reference collection at the University of Auckland.

Sequence of Events

We order our descriptions of features according to the following simplified sequence of events that was deduced from detailed mapping of the pit floor and walls: (A) earliest mineralization and formation of early structures: joints and faults, (B) clastic intrusions, (C) continued faulting, (D) major quartz vein development and mineralization, and (E) minor postvein faulting. The Discussion section provides a more detailed and expanded sequence of events.

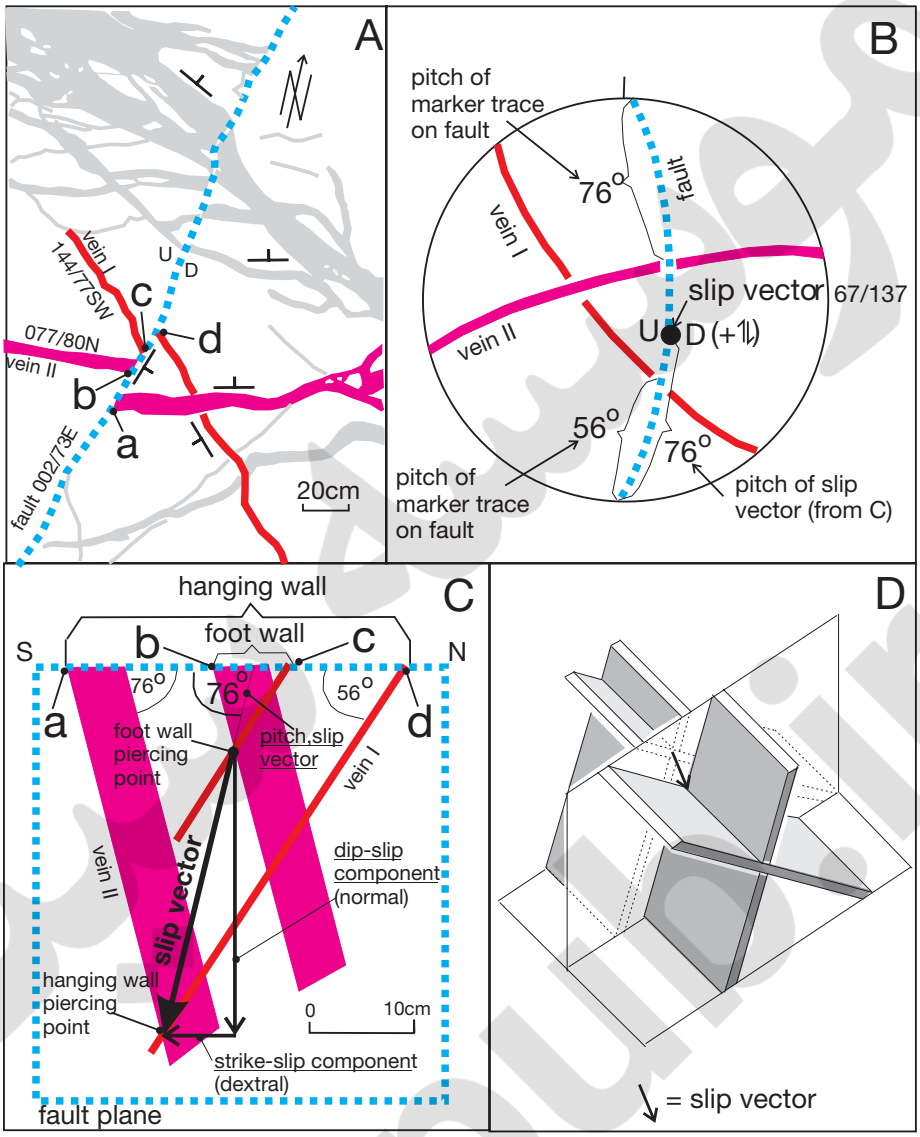

FIG. 6. Application of the piercing point method for a fault slip determination from two displaced markers at 1072.5 RL. (A) Map of outcrop dipping at a very low angle towards the observer. White = host rock, gray = quartz veins, except for the two marker veins which are shown in magenta and red colors. The fault is marked in blue. Important intersections of markers along the fault are labeled a–d. (B) Lower hemisphere equal area stereonet plot of the fault and the two marker veins. In this step, the two pitch angles of the traces of each marker on the fault plane (76° and 56°) are read off. (C) Construction of the slip vector: A view into the fault plane from the east (compare with (B)) to show the traces of the displaced markers constructed with the pitch angles from (B) and correctly positioned according to the spacings along a-b, b-c, and c-d in (A). The intersection of the two pairs of traces generates the foot wall and hanging wall piercing points. These in turn define the slip vector. The slip vector is then plotted back into (B), using the pitch of 76° measured in (C), allowing determination of its plunge and bearing of 67/137. (D) Schematic block diagram, not directly related to A–C, illustrating the three-dimensional geometry of a slip vector determination. The same method was used to obtain the slip on the large phase 2 fault at A in Fig. 5.

Early structures: Joints

Joints can provide important avenues for fluid flow in low-permeability rocks, and many veins at the Martha Hill mine were mineral-filled joints. Some joint patterns were complex, but others were more regular. For example, well-developed fractures in andesites on the south wall at level 1075 RL (Fig. 5) divided the rock into subparallel five-sided prisms (Cargill, 1994). We interpret these fractures as columnar cooling joints in the sense of Grossenbacher and McDuffie (1995). The basal planes of the prisms represent column-perpendicular fractures (see Schaefer and Kattenhorn, 2004). These had an average strike and dip of 008/30 E and should approximate the orientation of the margins of this tabular igneous body. This orientation is close to the 40° southeasterly dips of the tuff beds in the adjacent volcanic sequence (Brathwaite et al., 2006), suggesting that the igneous body was either a lava flow or a sill.

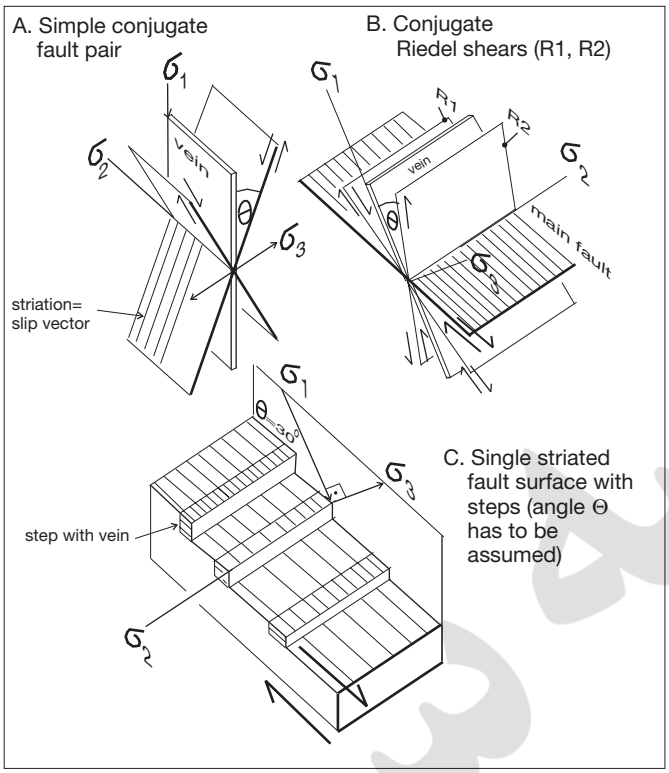

FIG. 7. Relationship of the three stress axes σ_1, σ_2, and σ_3 to faults and their slip vectors, after the principles presented by Anderson (1951), Beach (1977), Hancock (1985), Harding (1985), Pollard and Aydin (1988), Sylvester (1988), Rowland and Sibson (2004). Slip vectors in all the diagrams are shown by the parallel-ruled striations. (A) Simple conjugate faults; the angle θ is ½ the acute angle between the fault planes, and σ_2 is parallel to the intersection line of the two fault planes. (B) Conjugate Riedel shears with an oblique conjugate fault couple. (C) Single fault surface with striations associated with accretionary, fiber-veined steps indicating the sense of movement. Here, a value of the angle θ (e.g., 30°) has to be assumed.

Elsewhere in the mine there were joint sets in rectangular or triangular arrangements that also generated subparallel intersection lines indicating columnar joint patterns. Their joint surfaces varied from planar to curviplanar and some were stepped, similar to the hackle fractures described by DeGraff and Aydin (1987).

The andesites tended to be more pervasively jointed than the adjacent volcanic breccias. Some of the joints, although still present as open voids, had walls coated with chlorite and/or isolated euhedral crystals of pyrite. These, and associated pyrite/clay veinlets, represented the earliest mineralization.

Clastic intrusions

Tabular bodies of dark to medium gray granular material ranged from 1 to 40 cm in width and had lateral extents of up to tens of meters. These bodies, which we interpret as clastic intrusions, were mostly planar, displaying sharp contacts with the country rocks. Their strike varied from 345° to 060°, but north-northeast strikes were most common (Fig. 9). Dips were westerly, except for one measurement, and varied from 20° to vertical. However, if intrusion occurred prior to the eastward tilting in the volcanic host rocks, the lowest dips would originally have been steeper (about 60°) and more of the steeply dipping intrusions would have dipped to the southeast.

The grain size of the filling material varied from fine-grained sand to pebbles, with rounded to well-rounded clasts of igneous and sedimentary rocks. The very fine grained matrix of the intrusions consisted of the same materials. Sedimentary clasts were derived from a sequence of finely bedded, quartz-bearing, commonly carbonaceous sandstones and mudstones. Some of these clasts displayed arrays of closely spaced brittle faults truncated at the clast surface, indicating that this deformation predated their transport by the clastic

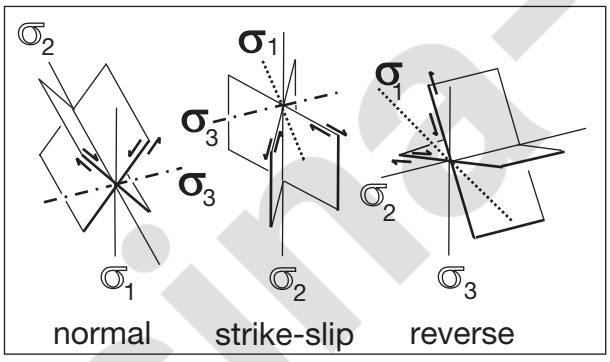

FIG. 8. Example of three co-axial but different conjugate fault couples that are kinematically compatible with each other to accommodate 3-D deformation, after Harding (1985) and Krantz (1988). Stress axes that are the same in two fault couples are labeled in solid black and are identified by broken lines. Coupled asymmetric arrows indicate orientation and sense of movement of slip vectors.

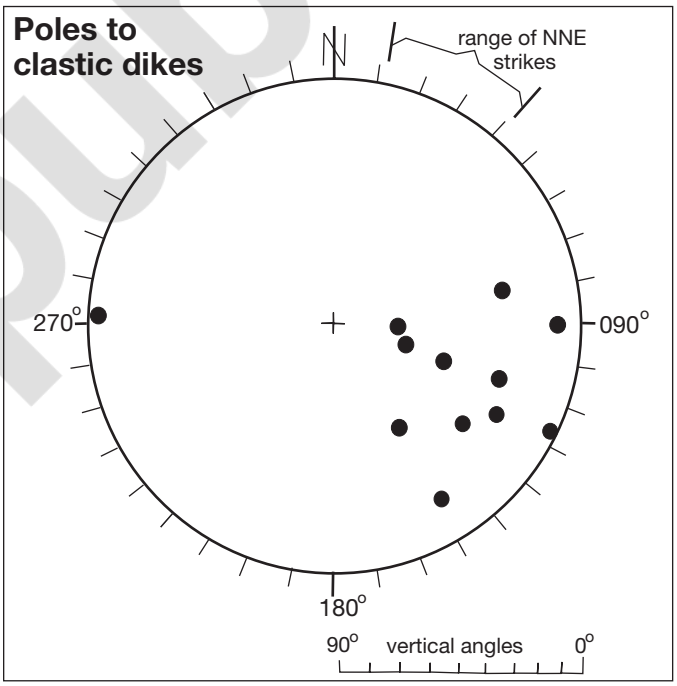

FIG. 9. Orientations of clastic dikes (also see Fig. 4A) plotted on lower hemisphere equal area net. Lowest dip is about 20°. Note the predominant north-northeast strikes and westward dips in the present orientation. This is opposite in direction to the dips of layering in the host volcanics. Restoring this layering to horizontal would increase the lowest dip to 60° and make more of the steep dikes assume easterly dips.

intrusions. The exact source unit of the sedimentary rocks is unknown (but see Discussion section). However, the low degree of lithification and lack of metamorphic veins precludes derivation from the Mesozoic basement rocks.

Textures within the clastic intrusions ranged from massive to layered parallel to the dike walls, with some graded layers and local lenticular cross-stratification. Coarser clasts tended to be concentrated behind protuberances in the dike walls, indicating flow-induced sorting on the lee side of these irregularities. The few flow features of this kind observed suggested upward or steeply oblique upward flow towards the north.

The clastic intrusions formed early in the sequence of events. While a few intruded into fault zones and therefore postdate at least some of the major faulting, most of them were cut by cross faults which were then displaced by faults subparallel to the their walls. All the clastic intrusions that we observed predated veining, however, a number of them have influenced the location and orientation of subsequently formed faults and veins.

Faults

Faults were the most important structural features controlling mineralization, commonly hosting the major veins (Brathwaite et al., 2006). However, because of the disruption of fault zones during vein opening, it was difficult to derive kinematic data from faults that were hosting major veins. Therefore, the data presented below were mostly collected from faults preserved between the veins. Qualitative comparisons with fault remnants along the veins indicate that the vein-hosting faults were similar to those studied in detail (Cargill, 1994).

Although the trace of the largest fault in the pit had a strike length that was greater than 400 m (Fig. 4A), most of the other faults were considerably smaller. Offsets were also small, ranging downward from about 50 cm, except for the fault at A in Figure 5, which had a total displacement of 22 m dominated by normal movement combined with a very small component of dextral strike-slip. None of the faults observed in the pit were regionally significant. Listed in order of importance, the following kinematic indicators yielded fault slip vectors: (1) striations (Fig. 7C; Table 1), (2) conjugate fault couples and Riedel shears (Figs. 7A, B, 8), and (3) offsets of two markers (Fig. 6).

Using the geometric relationships shown in Figures 7 and 8, we then grouped the faults with kinematic indicators according to their stress axis orientations (Fig. 10). From left to right, the diagram shows the following: (1) orientation, slip line and sense of movement of each fault, grouped into strike-slip and dip-slip sets where possible, (2) principal stress axes for all faults in a set, (3) idealized conjugate fault model for the stress axis pattern, adding any fault orientation not sampled in the field ("imaginary faults" of Shan et al., 2009) by assuming an acute angle of 60° between the two faults (lengthening dihedron shaded), (4) 3-D block diagram of the conjugate fault models, combining, where possible, compatible dip-slip and strike-slip models.

We recognize three groups of faults (their relationship to mineralization will be considered in the Discussion):

TABLE 1. Slip Lines (mostly striations) on 30 Faults in Martha Hill Mine

Fault strike + dip	Striation plunge + bearing	Striation pitch	Shear sense	Fault Group (see Fig. 10)
003/64 W	48/216	56 S	Normal/sinistral	A
006/64 W	53/219	60 S	Normal d.s.	A
172/74 E	54/016	58 N	Normal /dextral	A
160/30 W	29/264	79 NW	No steps, d.s.	A?
164/62 E	56/035	70 N	No steps, d.s.	A?
140/65 SW	60/263	74 NW	Normal d.s.	A
148/74 W	70/273	78 NW	No steps, d.s.	A?
141/48 NE	47/067	80 SE	No steps, d.s.	A?
005/70 NW	54/335	57 N	No steps, d.s./s.s.	B?
013/58 NW	65/313	70 NE	No steps, d.s.	B?
024/86 NW	64/016	64 NE	Normal d.s.	B
032/61 NW	38/006	46 NE	Normal /dextral	B
050/30 NW	29/304	76 NE	No steps, d.s.	B?
012/83 SE	49/020	49 NE	No steps, d.s/s.s.	B?
027/80 SE	44/037	45 NE	Normal /dextral	B
031/67 SE	54/067	62 NE	No steps, d.s.	B?
042/65 SE	59/171	70 SW	No steps, d.s.	B?
011/19 W	16/312	60 N	No steps, d.s./s.s.	B?
014/30 NW	24/324	54 N	No steps, d.s./s.s	B?
004/17 W	10/330	36 N	Dextral/normal	B
080/66 S	48/230	55 W	Reverse / dextral	B
085/vertical	70/265	70 W	No steps, d.s.	B?
049/83 SE	71/208	72 SW	Reverse d.s.	B
122/85 SW	10/123	10 SW	Sinistral s.s.	C
138/50 SW	08/311	08 NW	No steps, s.s.	C?
130/48 SW	05/305	08 NW	Sinistral s.s.	C
095/69 S	68/169	84 E	Normal d.s.	C
082/60 S	20/251	24 W	Dextral s.s.	C
080/60 N	31/280	36 W	No steps s.s./d.s.	C?
070/66 NW	18/257	19 NE	No steps, s.s.	C?

Measurements are in degrees; d.s. = dip-slip, s.s. = strike-slip, dominant mode listed first where applicable; also see stereonet in Fig. 4D

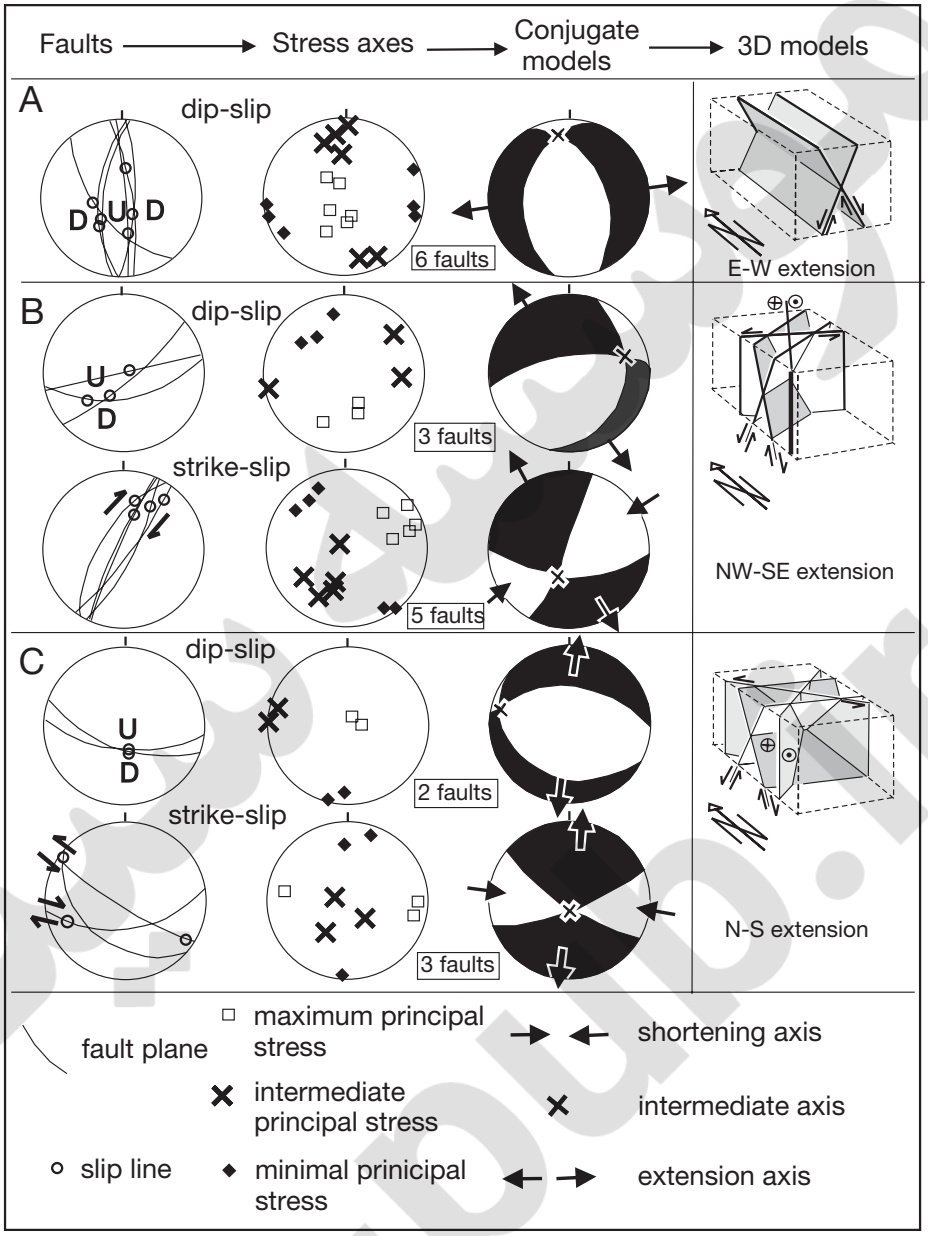

FIG. 10. Differentiation of fault groups A, B, and C after the steps shown in the heading of the Figure. All the large circles are lower hemisphere equal area stereonets. Assembly of the 3-D models in groups B and C was done following the principles for 3-D strain illustrated in Figure 8. Note the extension directions common between the normal and strike-slip faults in each of groups B (northwest-southeast extension) and C (north-south extension). In the 3-D models, small circles with a cross or a dot indicate strike-slip fault movement away from or towards the observer respectively.

Group A, normal dip-slip faults with ~east-west extension (Fig. 10A): The faults sampled are interpreted to be a conjugate set, with both east- and west-dipping faults. They include the major clay-filled faults that predate most of the veins, as well as some minor faults that postdate vein formation.

Group B, dip-slip faults (normal) and strike-slip faults, sharing northwest-southeast extension (Fig. 10B): In our sample, the strike-slip system is only represented by the northeast-striking dextral set where all slip vectors plunge gently to the north (the other, sinistral set of the conjugate couple would strike east-southeast). One east-northeast–striking normal fault crosscut earlier north-south–striking faults (Cargill, 1994).

Group C, dip-slip faults (normal) and strike-slip faults, sharing ~north-south extension (Fig. 10C): Among the normal faults, we have only sampled the south-dipping set of the potential conjugate couple. In the strike-slip group, both sets have been sampled.

Significance of the fault groups

Groups B and C, with their combinations of dip-slip and strike-slip faults, are typical examples of fault patterns indicating 3-D strain where there is deformation along all three strain axes. In contrast to this, the classical conjugate fault and mesh patterns (Sibson, 1996) and our group A represent 2-D

(plane) strain, where the intermediate strain axis is considered to be inactive. Groups A and C represent two perpendicular regimes of extension (~north-south and ~east-west), whereas group B, with its northwest-southeast extensional regime, is oblique to these. Integrating the larger faults, most of which have not yielded any information on their sense and direction of movement, into these groupings according to their orientation, the following correlations can be made:

Many of the faults in the pit (not shown in Fig. 4A) were parallel to or had a strike somewhat to the east of the general northeast-southwest trend of the Martha Lode and dipped steeply to the northwest. They may correspond to the northwest-dipping normal fault of the conjugate dip-slip component of the 3-D model in group B (Fig. 10) and, to a lesser extent, to the dextral fault of the strike-slip component in the 3-D model of group C. If the northeast-striking major lodes of the Martha Hill mine are dominantly extensional, they are most easily linked to the conjugate normal fault component of the 3-D model in group B.

A set of north-south–striking, steeply dipping faults with well-defined clay gouge/cataclasite zones crossed the open pit and was best seen on the north and south walls (Figs. 4A, 5). Their dip direction tended to change laterally and vertically. These faults correspond to the conjugate normal faults in model A of Figure 10.

A north-northeast–striking fault set (striking between 025°–040°) consisted of very steeply dipping, widely spaced faults and may correspond to the dextral strike-slip fault in model B (Fig. 10). An east-northeast– to east-striking (070°–090°) set included some prominent structures crossing the open pit, but also was represented by minor faults seen in the western and southern walls of the pit (Cargill, 1994). Faults in this set either correspond to the east-west–striking normal faults in 3-D model C (Fig. 10) or the east-southeast–striking sinistral strike-slip fault in 3-D model B (Fig. 10).

The faults crosscut the andesitic volcanic sequence and its cooling joints. Clastic dikes, though early, in some places appeared to be closely associated with and in some cases were subparallel to faults (Figs. 4A and 9). However, most faults cut the clastic dikes (Fig. 12) and predated the major veins.

Within fault populations there were some clear crosscutting relationships, such as the ~north-south–striking faults that predate an east-northeast–striking fault in Figure 5, but elsewhere there were conflicting age relationships, indicating more or less simultaneous movement and/or reactivation of older faults. Multiple fault movements also were indicated by more than one striation orientation on some fault planes, in some cases suggesting a change from oblique-slip to normal dip-slip with time.

Clear examples of faults that postdate veins were rarely observed (e.g., Fig. 6). All faults terminated against the unconformity below the overlying rhyolitic and sedimentary units (Fig. 5).

Most faults clearly resulted from brittle deformation, consisting of either a cataclastic fault zone or a narrow empty fracture. Textures in the cataclasites ranged from isotropic to foliated and included Riedel shear patterns (Figs. 7B, 11). Many of the approximately north-south–striking faults showed such cataclasites, but others had clay-dominated fault rocks. In contrast, northeast- to east-striking faults, if not occupied by veins, were marked by breccia zones.

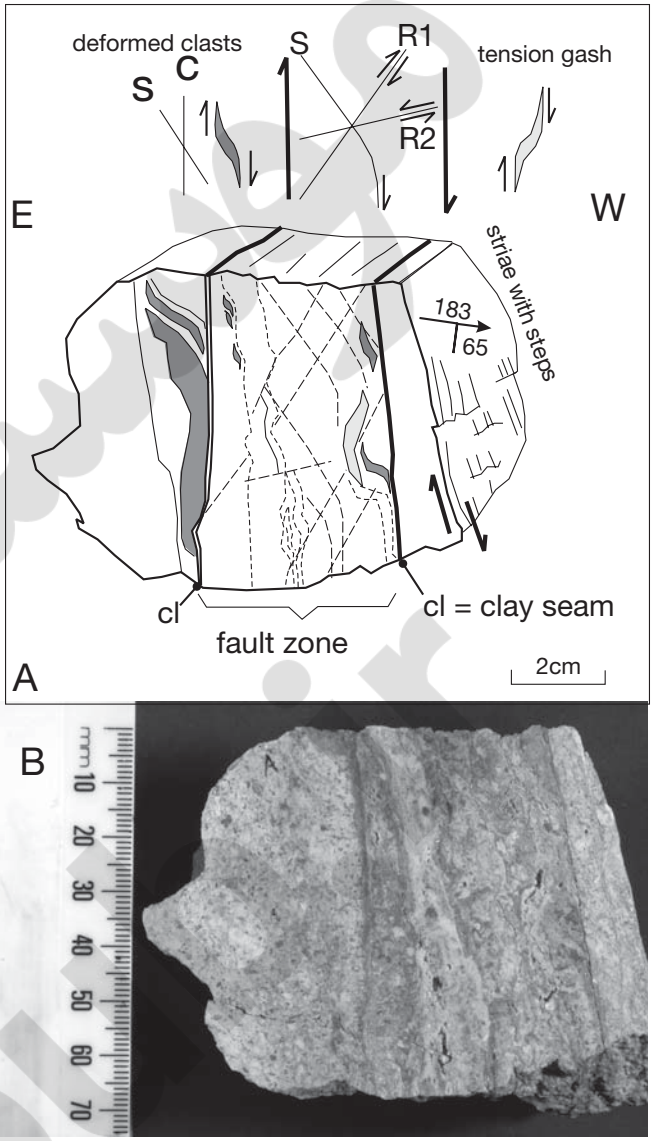

FIG. 11. Fault rock with brittle and ductile structures. (A) Simplified tracing of oriented sample AU45842 (see orientation mark on west side) of a fault zone with composite planar fabric, including striations, Riedel shears R1 and R2 (brittle deformation), and S-C structures (semiductile deformation). Structural geometries are shown above the specimen. Clay seams are at the boundary of the fault zone. (B) Photograph of the cut north face of the specimen.

Ductile structures were developed in clay-rich zones formed by hydrothermal alteration (Fig. 11) or in clastic intrusions. Some ductile structures displayed fabrics similar to mélanges (Fig. 12, also see Raymond, 1984) or to S-C fabrics in mylonites (Passchier and Trouw, 1998), and the clay-rich portions showed crude to well-defined internal layering of dark and light bands.

Locally, additional small shears oblique to the shear zone (R_2 shears of Hancock, 1985) that were inclined in the opposite direction to the S-surfaces dragged the S-C foliation, forming a "composite planar fabric."

In summary, our analysis indicates an extremely complex mesh of faults dominated by normal faulting with extension

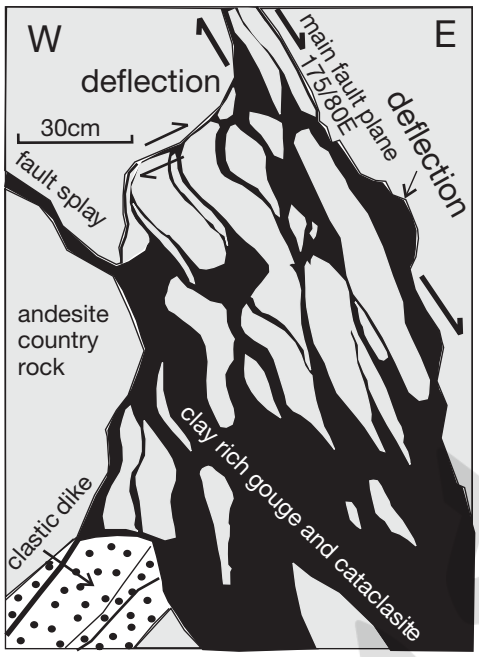

FIG. 12. Mélange-like internal structure of a fault zone showing asymmetric lozenges of country rock and deflections which indicate overall normal dip-slip movement. Note folding of the lozenges by drag on the antithetic fault below the scale bar. The zone also contains some fragments of cataclastically deformed vein quartz (not shown). At the lower left, a preexisting clastic dike is cut by the fault zone. Location: North wall of the pit at 1120 m RL.

directions in various directions. Some fault zones showed ductile behavior because their wall rocks and the deformed material between them had been weakened by hydrothermal alteration.

Veins

Vein mineralogy

The veins consisted primarily of quartz and lesser chalcedony, with minor adularia, carbonate, inesite ($Ca_2Mn_7Si_{10}O_{28}(OH)_2 \cdot 5(H_2O)$), pyrite, acanthite, and electrum. The general mineral sequence can be subdivided into three stages: early, main, and late (Christie et al., 2007), with quartz persisting in all three, calcite restricted to the early stage, and adularia and the sulfide minerals occurring in the early and main stages (Brathwaite and Faure, 2002). Electrum and acanthite were deposited only during the main stage, whereas inesite and amethystine quartz are late stage minerals (Brathwaite and Faure, 2002).

Vein textures

Vein textures arise from the variations in the state and composition of the mineralizing fluid (e.g., Dong et al., 1995). Some of these conditions, e.g., pressure, flow rate, turbulence, and direction of flow, may be linked to the structural controls of vein opening. Analysis of the nature, sequence, and geometry of vein textures, preferably in the orientation in which they formed, can therefore contribute to understanding of the structural development of a vein system.

In the part of Martha Hill mine examined, fills of individual veins ranged from single phases deposited symmetrically on the two vein walls to complex multiphase bands with a wide variety of gangue minerals and textures (e.g., Figs. 13, 14), including breccias of various types.

We recognized the following textures: comb quartz, crustiform textures, platy quartz due to replacement of platy calcite by quartz ("quartz after platy calcite"), cherty quartz, amethystine quartz, buck quartz (in barren to very low grade veins with interlocking euhedral to anhedral quartz), cellular quartz and saccharoidal texture (both due to leaching and dissolution of matrix materials), and breccias. The dark, sulfide-rich ginguro bands recognized below the 960RL level of Martha Hill mine by Martin and Mauk (2006) were absent in the upper portions we studied.

Breccias occurred locally, mainly within the larger veins. The following types were recognized: (1) jigsaw breccias mainly consisting of wall-rock fragments, (2) preexisting vein fill that had been disaggregated into a breccia of angular or

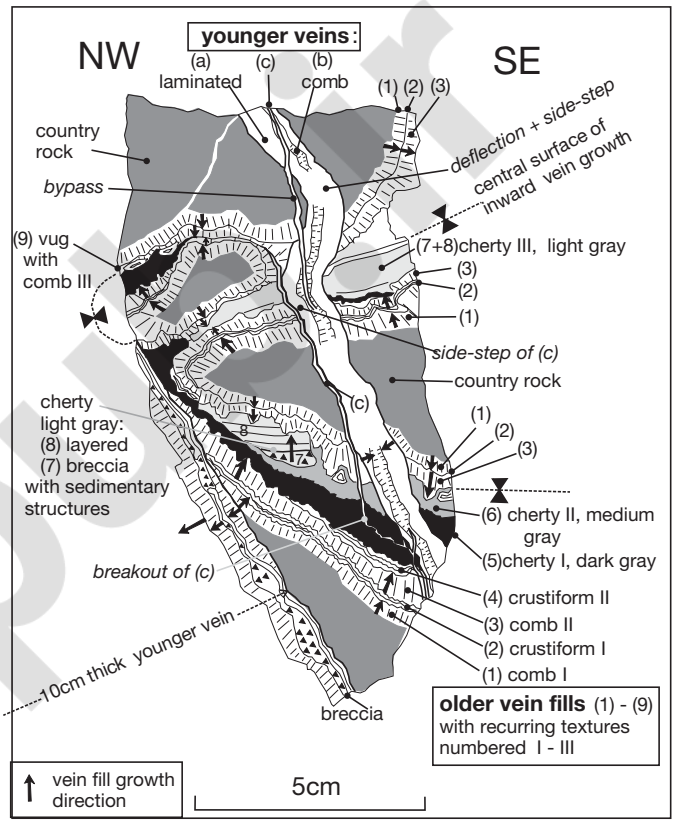

FIG. 13. Change from initial open space vein filling to fracturing and incremental opening during later stages of veining. Oriented sample AU45862. Country rock is a clastic dike. Numbers 1–9 indicate position within the general sequence. Numbers I–III count the recurrence of one particular type of texture. The bands of phases 1–4 are typical of the gold-bearing vein fills elsewhere in the mine. The central surfaces of inward growth in vein fills (bow tie symbols) are based on opposing growth directions determined from cusps in botryoidal contortions, crosscutting between layers, and sedimentary structures in the cherty layers. Some of the growth patterns are not symmetrical because of an episode of vein fill removal. Note the deflection of the second phase vein with fills (a) and (b) in the top half of the specimen, breakout and bypass of latest veinlet (c). Influx of the cherty material marks a significant fluctuation in physico-chemical conditions in the mineralizing fluid.

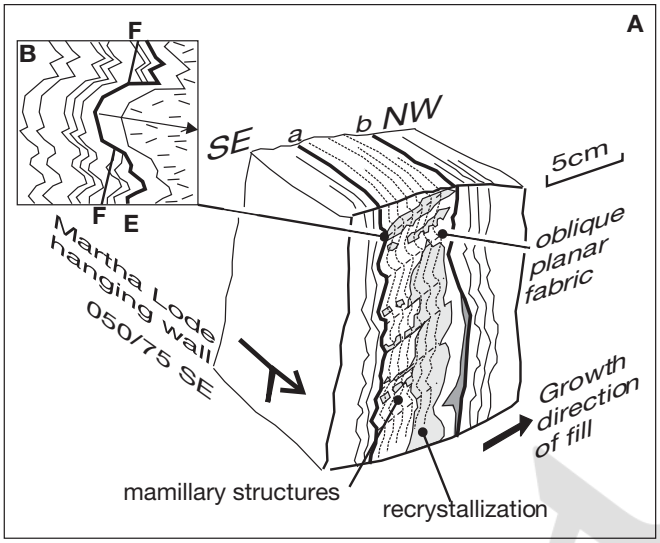

FIG. 14. Vein specimen illustrating persistence of an open fissure over time. (A) Sketch of oriented sample AU 45859 near the hanging wall of the Martha lode (for location see Fig. 4A) with erosion surfaces (a) and (b) and persistent mamillary textures forming planar fabric oblique to the vein wall. (B) Thin section view of erosional and depositional truncation of fracture F on surface (a), indicating the vein fill growth direction (arrow) and suggesting a notable time interval for formation of this contact.

rounded clasts, (3) noncemented vein breccias that were caused by leaching of components and/or late faulting. While all three types can be explained by rock falls in open fissures, hydrofracturing or fault zone brecciation is likely, especially in types (1) and (3).

Variations in orientation and/or thickness in a vein were locally accompanied by changes in vein fill textures. For example, quartz-after-calcite bladed textures dominated in wider segments of veins but were less significant in the thinner segments. Furthermore, east-, north-northeast– and north-striking veins tended to display fewer textural types and generations of vein fills than the wider veins that form the main northeast-striking lodes.

The variety of textures described above indicates that repeated changes in the physical and chemical conditions of the mineralizing fluid accompanied multiple episodes of vein opening and sealing that were influenced by extensional tectonic events and by the configuration of the vein walls inherited from preexisting structures.

Sequence of textures during vein filling

The Martha vein displayed complex banding, with multiple cycles of complete sealing of the vein followed by renewed fracturing, opening, and mineral deposition. Cherty material tended to be deposited late in a cycle. Detached "horses" of country rock in the center of the vein suggest that the main lode tended to grow by the widening of thinner peripheral veins, consistent with the observation of Martin and Mauk (2006) that thin veins tend to predate the thick veins. Many of the thinner veins bifurcated upward, but some also diverged downward (Fig. 15). Deflections were very common. Preferential occurrence of breccias and formation of the latest vein phases may indicate that the last opening and filling event took place along the footwall of the Martha Lode.

Corresponding processes are also detectable at the hand specimen scale, such as that shown in Figure 13. In this example, the host rock, a clastic dike, was initially brecciated to provide the voids for the first stage of mineral deposition. These voids were held open long enough to allow a complex sequence of deposition of comb and crustiform quartz (Fig. 13, phases 1–4), followed by erosion and influx of cherty material with sedimentary structures (phases 5–8), and back to comb quartz (phase 9), which completely filled any still remaining spaces.

This consolidation allowed fractures of the second stage of veining (veins (a) and (b) in Fig. 13) to cut straight across the rock fabric. Laminated vein fill and comb quartz sealed the fractures and the 10-cm-thick vein on the northwest side of the specimen was formed.

In a third fracturing and vein-filling sequence, quartz veinlets (c) opened along veins of the second stage but formed some breakouts as described by Gadsby and Spörli (1989). This again left the rock mass completely cemented.

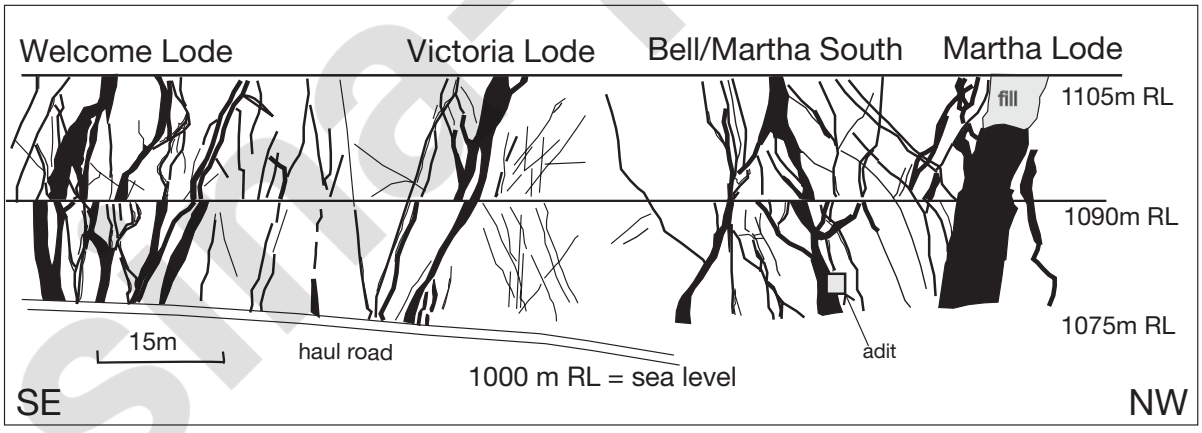

FIG. 15. View of the western pit wall, with medium and large size quartz veins in black and country rocks white. For location, see Figures 4A and 5. Note branching and opposing dip directions of individual veins within the various vein systems.

Subtle mechanical controls by the host rock are indicated by the following: (1) The vein with fills (a) and (b) cuts straight through the lower segment of earlier vein fill (phases 1–9 in Fig. 13), but sidesteps and deflects across the upper segment, indicating that the latter was a barrier to fracture propagation during formation of veins a and b. (2) In contrast, the latest veinlet (c) sidesteps and deflects in the phase (5) cherty material of the lower segment and forms a straight "bypass" across the upper segment.

This specimen illustrates three different modes of mineralization: (1) deposition in preexisting cavities that remained open for a certain length of time (Phases 1–9), (2) mineralization of new fractures (phases (a) and (b)) recutting a previously cemented material that does not have much control on the propagation direction, and (3) propagation of vein-hosting fractures (veinlet (c)) controlled by preexisting mechanical discontinuities. Persistence of an open fissure over some time is also indicated by the multiply banded crustiform vein fill with mamillary textures and the presence of two erosion surfaces in the specimen shown in Figure 14. These processes can also be seen in the larger veins.

Vein patterns (Figs. 4A and 15)

At the levels investigated, the vein system formed a rectilinear, up to 100-m-wide block elongated over 360 m in a northeast-southwest direction. The veined block consisted of many large northeast-striking veins with strike and dip lengths of tens to hundreds of meters and thicknesses of 10 cm to several meters; these large veins were interconnected by a stockwork of smaller veins. In the north (Fig. 4A), the vein block was mainly bounded by the major, up to 30-m-thick Martha Lode, which has a known strike extent of 1.7 km and contained Au ore for 650 m in the vertical dimension. The Martha Lode formed the footwall of the veined block. In the south, the boundary was more diffuse, but the Welcome Lode (Brathwaite et al., 2001) was prominent in this zone. Most of the veins in the array dipped steeply to the northwest except those along the northern boundary, which dipped steeply southeast. The Victoria Lode also had mostly southward dips. There was a significant group of east-southeast–striking veins and a few north-south–striking veins. The width of the veined block narrowed downward as other veins converged with the Martha Lode. Brathwaite and McKay (1989) estimated that the then-visible Martha Hill mine block had been dilated by about 10 percent by volume, corresponding to precipitation of 0.05 km^3 of quartz. Brathwaite et al. (2001) measured larger dilations of 16 to 21 percent.

The steeply southeast-dipping Martha Lode deflected from a 050° to a 070° strike (Fig. 4 A) on a line plunging 70° to the southeast (Fig. 4C). It had two splays, the 080°-striking north branch and the south branch. The deflection approximately coincided with the junction of the north branch with the main vein and was marked by local splay patterns.

The Welcome Lode was divided into three segments separated by two pronounced left steps (Fig. 4A). While the western and eastern segments dipped steeply northwest, the middle segment dipped southeast. Each of the left steps coincided with north-south–striking faults (Fig. 4A), which presumably predated the Welcome Lode and acted as barriers for the lateral propagation of the vein. It is important to distinguish such sidesteps (Beach, 1977; Hancock, 1985; Pollard and Aydin, 1988) from fault offsets of a vein because of the opposing implications for the relative timing of the structures. The lack of sidesteps along the Martha Lode may reflect a different time of vein formation, or more likely, the greater force of the opening events for this major vein structure.

The Victoria Lode (Figs. 4A, 15), with an average strike of 075° and steep dips to the south, is a splay of the Welcome Lode, which it joined in the center of the middle segment. Toward the west, the Victoria Lode bifurcated into a horsetail. The veins in this system were commonly sigmoidal in plan and displayed fewer vein phases of vein fill than those in the Martha and Welcome systems.

In the Bell vein system (Fig. 4A), the main veins dipped steeply to the northwest, but some nearby parallel veins had steep southerly dips. A prominent left step was also sigmoidal, with an axis plunging 70° to north-northeast and included an angle of 40°, much smaller than the 75° of the Welcome Lode sidesteps.

Analysis of orientations of the veins between the main lodes indicates that most of them dipped to the northwest (Fig. 4B). The rose diagrams of all defect strikes (Fig. 4A) display prominent maxima at 0°, 040°, 060°, 080°, and 100°. While the northeasterly strikes were more prominent near the pit floor, east-southeast strikes became prominent farther out in the pit walls. The summary rose diagram of veins (Fig. 4A) is dominated by the northeast strikes.

Despite the great variety in orientations, the vein patterns were clearly dominated by northeasterly vein strikes. Complexities in the main veins included changes in dip direction, deflections, sidesteps, sigmoidal shapes, and bypass structures. These arose from control by preexisting structures and variations in amount of extensions during opening of the veins. Little is yet known about what influence these perturbances in the vein pattern had on fluid circulation and ore deposition.

Geometrical description of vein deflections can contribute to understanding of the stress-strain framework and the hydraulic geometry of a vein system (e.g., Nortje et al., 2006). Vein deflection axes are lines marking relatively low angle changes in orientation along a vein, subdividing it into differently oriented segments (Gadsby et al., 1990; Spörli et al., 2006). Some of these are probably analogous to segmentation of faults (Kattenhorn and Pollard, 2001; Mansfield and Cartwright, 2001) which may involve linkage of separately nucleated, slightly displaced fracture segments. In the portion of Martha Hill mine examined, 60 percent of the vein deflection axes plunge steeply, and although there are also a number of low angle lines, none of them are horizontal. The most common deflection angles lie in the 30° to 40° range. Deflection lines in the southwestern part of the veined block displayed both northerly and southerly directions of plunge, whereas in the southeastern part, they consistently plunged west to west-southwest. The vein deflection pattern at the Martha Hill mine is more complex than that described from Karangahake and Broken Hills, where nearly all the axes plunge steeply (Gadsby et al., 1990; Nortje et al., 2006), which may indicate that there was greater connectivity of flow paths for the hydrothermal fluids at Martha.

Sequence of vein formation

Fifty crosscutting relationships of small scale stockwork quartz vein pairs were collected (Fig. 16). The poles form four overlapping clusters representing two sets of orthogonal directions: (1) northeast- and northwest- and (2) north- and east-striking sets of veins (Fig. 16A). Except for the northwest-striking veins, all the sets contain members with opposing dip directions. The arrangement of vein sets into two orthogonal arrays—northeast- and northwest-striking and north- and east-striking—is similar to that seen in the fault arrays (Fig. 10) and presumably represents two pairs of orthogonal extension directions.

Figure 16 B–F shows groups of similarly oriented vein pairs with similar sequences of formation:

Figure 16B: Northwest-striking veins predate other veins.

Figure 16C: East-striking veins predate north-striking veins.

Figure 16D: Northeast-striking veins predate both east- and north-striking veins.

Figure 16E: In some places, we could constrain three generations of veins, as indicated by the numbering and gray arrows. East-striking veins postdate north-striking veins and northeast-striking veins are the youngest.

Figure 16 F: Among the northeast-striking veins, steeply northwest-dipping veins formed before the southeast-dipping set. A bimodal array of poles at X and Y indicates formation of a deflection pattern in these later east-dipping veins. We have not found any such progression for the other vein sets.

Taken together, multiple crosscutting relations in Figure 16B–F confirm that in the stockwork at Martha Hill mine there was alternation of opening between sets of veins striking in different directions. For such alternations there are two end-member interpretations: (1) all the vein directions were opening more or less at the same time and the crosscutting relationships are only small incremental steps in an otherwise simultaneous overall process, or (2) the crosscutting relationships represent an actual, but very complex, sequence of events. The real situation may be a combination of these two scenarios. On one hand, the dominance and persistence of the northeast-striking Martha and Welcome veins, indicating that they were active until the cessation of vein formation, favor an overall main sequence of northwest → east-west → north-south → northeast-striking veins (Fig. 16C, 16E). On the other hand, the contradictory relative age data in Figure 16C–E indicate that in detail there was some oscillation between the various vein directions during this general development.

Discussion

To set the observations presented above into an overall context, we tabulate (Fig. 17) and discuss the geological history seen in the upper part of the Martha Hill mine deposit and then consider the nature of faulting, clastic intrusions, and veining. We discuss the significance of vein fills, vein patterns in space and time, and structural control of the veins. Important points are: (1) control of veining and mineralization by preexisting low-displacement faults, (2) the complexity of vein and fault orientations despite the dominant northeast strikes, (3) a preponderance of normal dip-slip faulting, indicating an extensional regime, (4) eventual concentration of opening strain into a very small number of veins, among which the Martha Lode reached thicknesses of up to 30 m, (5) occurrence of 3-D (non-plane) strain. In a final section, we make comparisons with other epithermal deposits in the Hauraki goldfield and elsewhere and discuss possible tectonic controls for the mineralized veins.

Overall sequence of events

Figure 17 presents the detailed sequence of events that emerged from our study of the uppermost Martha Hill mine in the context of local and regional geology over the last 8 Ma. Events at Martha Hill mine are bracketed between the deposition of the Waipupu Formation andesitic host rocks at about 7 Ma and that of the Black Hills dacite at about 5 Ma (Brathwaite and Faure, 2002). Quartz-pyrite veins, the clastic intrusions, and the major faulting preceded the main pulse of epithermal mineralization, which occurred at 6.16 ± 0.06 Ma (Mauk et al., 2011). The Black Hills dacite overlies an important postmineralization erosion surface. Including formation of the present day relief, three periods of erosion have affected this area since the formation of the Martha Hill mine deposit.

Faults

All the faults accessible to detailed study were only locally significant, with displacements generally less than 0.5 m. Displacements on the faults that host the larger veins could not be determined because of the lack of stratigraphic markers in the host volcanic rocks.

Crosscutting relationships show that most faults were initiated at some time between the intrusion of clastic material and opening of the veins. However, some faults postdate some veins (e.g., Fig. 6A), so the main faulting episode must have preceded mineralization and overlapped with it, and faulting and veining were part of the same event. While there is some evidence that ~east-west–striking faults (Group C in Fig. 10) preceded the northeast-striking faults (Group B in Fig. 10), mutual crosscutting relationships favor simultaneous movement on a network of differently oriented small-displacement faults.

At the Martha Hill mine, there is no evidence for large scale strike-slip faulting as invoked for some other deposits (e.g., Berger et al., 2003; Chauvet et al., 2006), and in particular, not for regional north-south–trending dextral strike-slip faults required by the extensional jog models for the Martha Hill mine suggested by Wellman (1954) and Sibson (1987). The prominent north-northeast–striking East Fault (Fig. 2) east of the mine predates the vein system (Brathwaite et al., 2006) and its slip is unknown. If all the faults that provided slip vectors in our study are considered, dip-slip faults were much more common (77%) than strike-slip faults (23%) (Table 1). Therefore, we conclude that the Martha Hill veins formed in an area that was dominated by northwest-southeast extension and dip-slip deformation.

We recognized three groups of faults: (1) a group with east-west extension (Fig. 10A), (2) an orthogonal group with north-south extension (Fig. 10C), and (3) a group with northwest-southeast extension (Fig. 10B). In all three groups, two of the strain axes lie very close to the present-day horizontal plane, which suggests that there has been little tilting since the formation of the fault arrays. The orthorhombic arrays of

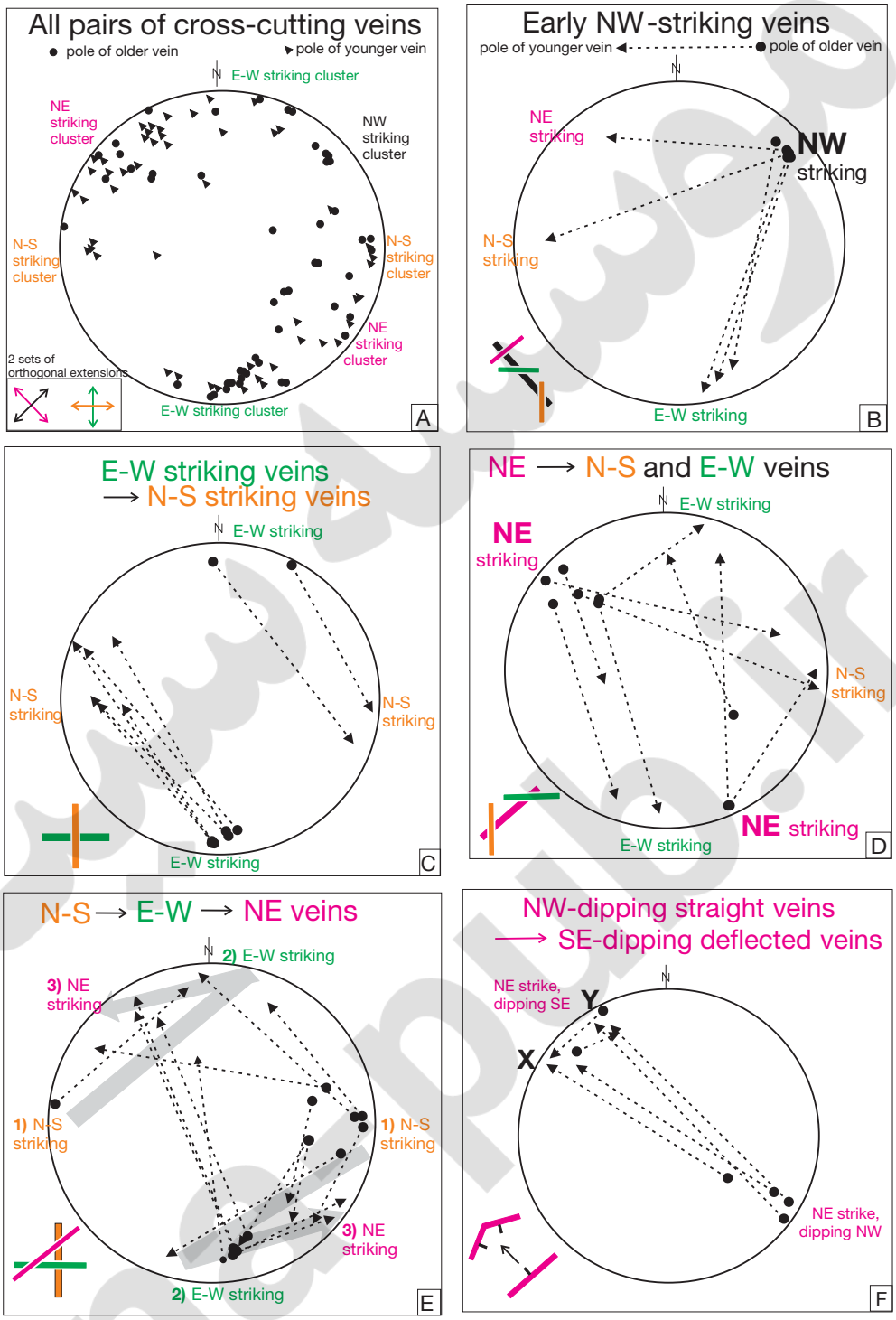

FIG. 16. Factoring out meaningful patterns from a complex vein sequence. Based on 50 small-scale crosscutting relationships between stockwork vein pairs from Cargill (1994), shown on lower hemisphere equal area nets. Note that these are vein orientation data in addition to those shown in Figures 4 B and C. The vein directions are color coded. (A) The total set of 50 vein pairs. Vein clusters are labeled on the periphery of the net. Corresponding orthogonal extension groups are shown in the lower left hand corner. Starting out with a plot like A, compatible vein pairs were separated out for Figures B to F, where arrows indicate the relative age of veins and the colored bars in the left hand lower corner show crosscutting of the veins. (B) Northwest-striking veins predating all the other sets. Note that these veins only dip to the southwest. (C) One of the two age relationships between north-south–striking and east-west–striking vein sets. Each vein set has two opposing directions of dip, as is the case in Figures D to F. (D) The dominant northeast-striking veins predate east-west– or north-south–striking veins. (E) Sequence of three events, shown by gray arrows and numbering. Here the dominant northeast-striking veins postdate east-west– and north-south–striking veins, opposite to Figure C. (F) Northeast-striking veins with a progression from northwest-dipping to southeast-dipping and separation into two clusters, X and Y, indicating deflection.

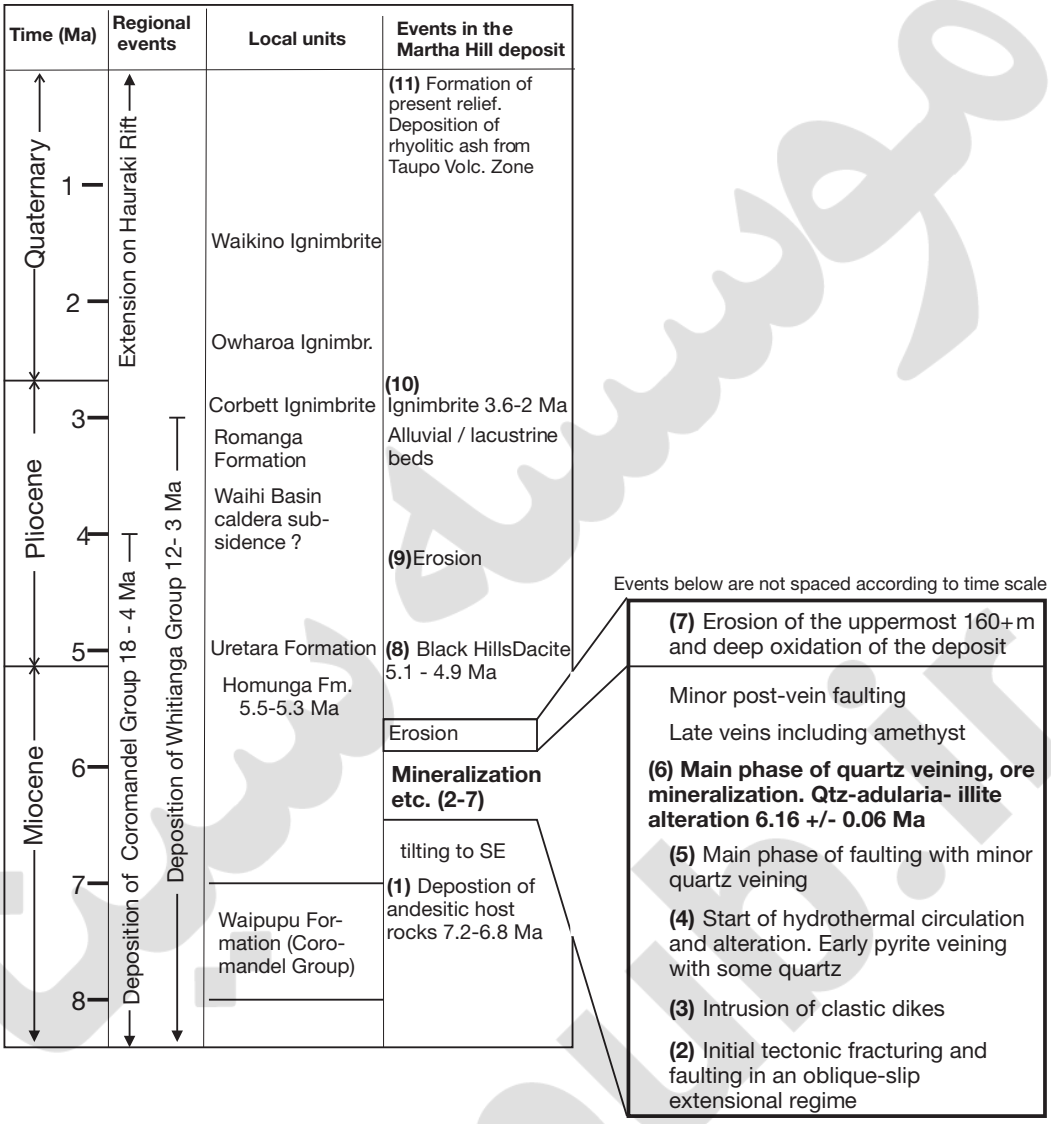

FIG. 17. Sequence of events in the Martha Hill mine in relation to regional geology, after Brathwaite et al. (1986), Brathwaite and Faure (2002), Smith et al. (2006), Christie et al., (2007), and Mauk et al. (2011). Bracketed numbers in the third column correspond to sequence numbers in the Conclusions section.

faults in Figure 10B and C indicate 3-D (non-plane) strain, where deformation occurred via all of the three strain axes, allowing extension in more than one direction (also see "Methods and Sources of Data"). Such 3-D strain most likely occurs where the difference between the principal stresses is small and/or the deforming body is irregular, either due to the interference of different structural directions, inhomogeneity of material or structural framework (e.g., in a caldera or a dome), or due to the influence of topography at shallow levels in the crust (Spörli et al., 2006). This 3-D strain can also occur in linkage regions between fracture segments (e.g., Rowland et al., 2007). Some of the faults in Martha Hill mine display ductile deformation due to local weakening of the rocks caused by intrusion of clastic material and/or hydrothermal alteration (Fig. 11). While this may facilitate opening of such weakened zones during later tensile fracturing associated with vein formation, the smearing out of clay-rich material may also make a fault zone less permeable, changing it from an aquifer into an aquiclude, and thus altering the flow patterns in the rock mass.

Veins

Vein textures indicate two contrasting mechanisms of vein filling: (1) cycles of incremental fracturing followed by filling of the openings and (2) volumetrically minor fill of long-lived static cavities (Fig. 13). Although some of the thinnest veins may represent a single opening event, thicker ones, especially the Martha and Welcome Lodes, experienced numerous incremental steps of opening.

In mechanism (1) a vein will be built up by a number of bursts of incremental opening and subsequent filling, either driven by earthquake fracturing (Sibson, 1987, 1996) or by hydraulic fracturing controlled by hydrothermal processes only (Jébrak, 1997; Browne and Lawless, 2001). Mechanism

(2) requires relatively long-term persistence of open fissures and is somewhat similar to deposition of wall coatings in limestone caves (e.g., Ford and Williams, 2007), leading to formation of deposits associated with local sedimentary structures (troughs, bedding etc.) and breccias due to gravitational detachment and collapse of the vein walls. Mechanism (1) could be more conducive to transport of large volumes of fluid, whereas mechanism (2) may favor lower volume flow. Although both mechanisms contributed to filling of veins, we emphasize that mechanism (1) is by far the most important at the Martha Hill mine and at other adularia-sericite deposits worldwide.

The veined zone in the Martha Hill mine dips about 75° to the southeast and persists in width at depth (Fig. 3). Layering in the Coromandel Group volcanics also dips to the southeast, at about 40°. If the veined zone formed when the layering was still horizontal, its initial dip would have been 35°. Such a low dip on a major zone of mineralization is atypical for adularia-sericite epithermal deposits in the Hauraki goldfield and elsewhere, so we agree with Hobbins (2009) that the vein system formed in its present orientation after tilting of the volcanic host rocks.

The northeast-striking veins were clearly the main veins in the area, as indicated by their abundance, thickness, lateral and vertical extent, and their importance in the gold production (Fig. 4). Among these, the Martha and Welcome Lodes are master structures, and they also mark the boundary of the main veined block (Brathwaite et al. 2006; Fig. 5). It is possible, but not proven, that their controlling faults marked a local northeast-striking graben structure. An important question is how they came to be preferentially developed into thicker veins. Partitioning of vein formation into these zones may have been facilitated by a particularly low strength of the preexisting controlling faults, leading to larger fluid inflow during suction events such as those proposed by Sibson (1987). In addition, a change with time from distributed fracturing to localized fracturing along the borders of the array, such as described by Soliva and Schultz (2008), may also have played a role in the preferential development of the Martha and the Welcome Lodes.

In the complex vein mesh of the Martha Hill mine, the northeast-striking veins predominated at the larger scale, but the smaller scale stockwork veins showed several different orientations (Fig. 16A). These orientations can be grouped into two arrays of orthogonal veins, one with northeast-southwest and northwest-southeast strikes, and the other with east-west and north-south strikes. The northwest-striking veins formed early (Fig. 16B). Later, opening oscillated between all the vein sets, indicating more or less simultaneous development. However, the sequence north-south → east-west → northeast (Fig. 16E) must have predominated, which eventually allowed the Martha and Welcome veins to develop their full width and persistence.

The north-south–, east-west–, and the northeast-striking sets each had veins dipping in opposite directions (Figs. 15, 16). These match the orientations of the three sets of conjugate couples recognized among the faults (Fig. 10), indicating that the veins were following preexisting faults instead of bisecting a contemporaneous conjugate fault couple, as would be expected in an extensional jog array (Fig.7A, and Hancock, 1985). For example, the Victoria Lode is continuous with a fault to the east (Fig. 4A), and some of the faults studied in detail (Fig. 4D, Table 1) are parallel to dominant vein orientations. The intricate branching patterns of the veins at several scales (Figs. 4, 6A, 15) also indicate replacement of a complex fault array. This is supported by the observation of Brathwaite et al. (2006) that the Martha, Empire, and some other lodes (e.g., the Welcome Lode in Figure 5) have faults along one of their walls. As a result of the replacement of an especially complex fault mesh, the distribution of deflection axis orientations in our study area is more complex than that described from elsewhere in the Hauraki goldfield (Gadsby et al., 1990; Nortje et al., 2006).

Therefore, a mechanism by which faults with initial movement parallel to their walls (shear mode, e.g., Pollard and Aydin, 1988) later opened as veins by joint-like movement at high angle to their walls (opening mode, Pollard and Aydin, 1988) contributed to formation of the Martha Hill mine deposit.

Of the extension directions deduced from the vein clusters (Fig. 16A), all except the northeast-southwest direction (Fig. 16A, B) were also recognized in the fault patterns (Fig. 10). This indicates that the orientations of the axes of horizontal strain were generally maintained from formation of the faults to the opening of the veins, suggesting that faults and veins were part of the same evolving process. Although the tectonic significance of these multiple extension directions is not yet completely understood, the northwest-southeast/northeast-southwest orthogonal extension couple includes the general northwest-southeast opening direction of all the major veins in the southern goldfield (Figs.1, 2; and Mauk et al., 2011). Therefore, although there was local multidirectional extension, the maximum amount of opening and of mineralization occurred on the northeast-striking veins represented by the Martha Lode.

Significance of the clastic intrusions and their mode of formation

The dominance of gray clastic sediments in the clastic intrusions suggests a link to the carbonaceous clastic units intercalated with some of the volcanic sequences in the area, such as those found in the late Miocene Waipupu Formation (Fig. 17) of the Coromandel Group (Brathwaite et al., 2006). Small scale faults within some clasts indicate that some of the source sediments were consolidated and had experienced deformation prior to being swept into the clastic intrusions.

Clastic intrusions can form (1) during sedimentation (Cosgrove, 2001), (2) associated with igneous intrusions (Andrews, 2003), (3) associated with hydrothermal venting and brecciation (Egan and Ashley, 1992), and (4) during earthquakes (Munson et al., 1995). The clastic intrusions show no sign of being directly involved in the sedimentation of the immediately surrounding deposits. No connection with any igneous activity such as dikes or sills was detected, nor is there any igneous signature in the matrix of the intrusions. Such clastic intrusions have not been described from other epithermal Au/Ag deposits in the Hauraki goldfield. The intrusive "muddy breccias" in the Kelian gold deposit, East Kalimantan, display some similarities but are different in that they are much larger and very irregular bodies with a number of

breccia facies and are clearly linked to a maar-diatreme complex (Van Leeuwen et al., 1990; Davies et al., 2008a, b). There is no connection of the Martha Hill mine clastic intrusions with the hydrothermal activity of vein formation, which clearly postdates them. We therefore conclude that the simple geometry and content, as well as the close association of the clastic dikes at Martha Hill mine with faults, favor a tectonic, earthquake-triggered origin and indicate transient high fluid pressure conditions.

Comparison with other deposits

The formation of adularia-sericite epithermal orebodies reflects many different structural and tectonic controls at local and regional scales (e.g., Sillitoe and Hedenquist, 2003). This section focuses first on local structural controls in the Hauraki goldfield and elsewhere, and then on regional scale tectonic controls in adularia-sericite epithermal districts outside New Zealand, with final consideration of regional tectonic influences that may have affected the Martha Hill deposit.

Local structural control, Hauraki goldfield

The 200-m-wide vein array in the Martha Hill mine is more complex than other mineralized vein systems within the southern Hauraki goldfield. So far, only two deposits with economic stockworks have been identified in the goldfield: Martha Hill and Golden Cross, but both deposits contained most of their Au resources in large veins (Brathwaite and Faure, 2002; Begbie et al., 2007). The Golden Cross deposit contains a master vein associated with en echelon type "footwall" veins; the master vein and footwall veins have been tilted by 50° to the southeast. A separate late-formed stockwork of thin, simple suborthogonal veins formed in an array adjacent to the master vein before and after tilting (Begbie et al., 2007). In contrast, the stockwork at Martha Hill contains an intimate mix of major and minor veins that formed more or less simultaneously or preceded the formation of the major lodes such as Martha and Welcome; all veins at Martha Hill likely formed after tilting.

Many of the deposits in the southern Hauraki goldfield have relatively simple geometries, and opening of these veins approaches 2-D (plane strain) deformation (Spörli et al., 2006). For example, at Favona, mineralization is dominated by a 1- to 3-m-wide vein that extends more than 1000 m horizontally and 400 m vertically along a fault system; it terminates in the classical upward diverging pattern seen or inferred in many epithermal vein systems (Fig. 2; Simpson and Mauk, 2007). The Jubilee and Sovereign deposits ~4 km west of Martha Hill mine are also single, steeply dipping veins no more than 1 m wide that follow faults (Haworth and Briggs, 2006). At Karangahake (Fig. 1), two west-dipping veins, the Maria vein (average thickness 2–3 m) and the Welcome-Crown vein (thickness up to 1 m) dominate (Stevens and Boswell, 2006).

The northern Hauraki goldfield mostly contains deposits that reflect 2-D strain, but there is also evidence for 3-D strain. For example, the Hauraki mine has two orthogonal vein sets that strike north-northeast and east-southeast, and also some minor northwest-striking veins, which indicates true 3-D strain (Spörli et al., 2006). In contrast, the Tokatea Reef near the Hauraki mine (Skinner, 1986; Christie et al., 2007), which strikes northwest over a distance of at least 6 km, again represents plane strain.

Taken together, the available data lead us to conclude that the controls that cause 3-D opening of the vein systems in the Hauraki goldfield must be of a relatively local nature. Future work could address whether 3-D strain, which causes more multidirectional and complex vein geometry and connectivity, enhances or diminishes the potential for ore endowment of a deposit.

The overall northeast strike of the vein system at the Martha Hill mine deviates by ~ 30° clockwise from the north-northeast strikes of most other veins in the area (Christie et al., 2007), but some north-northeast–striking veins do occur within the Martha Hill mine system. On the other hand, portions of the vein system at Favona, and the Maria and the Welcome veins at Karangahake, deflect into a northwest direction, corresponding to minor vein strikes within the Martha Hill mine system. This indicates that several directions of defects were available for vein opening in the Hauraki goldfield, but a combination of local structural control and the general extension direction determined vein geometry at each site.

The fault-vein age relationships seen in the outcrop at the Martha Hill mine, and the fact that veins follow fault surfaces instead of being en echelon to them, indicate that some veins exploited networks of preexisting faults. Therefore, the variations in orientation and degree of complexity of vein patterns at Martha Hill may be due to local variations in the preexisting fault meshes exploited by the vein opening during general northwest-southeast extension.

Local structural control outside New Zealand

Worldwide, adularia-sericite epithermal deposits form in a variety of structural settings. Strike-slip faulting has been established or proposed at several deposits. (1) Faults with well developed dextral strike-slip indicators control the mineralization in the Mesquite district, California (Willis and Tosdal, 1992). (2) The structurally simple, three-phase Santo Niño silver-lead-zinc vein of the Fresnillo district in Mexico is attributed to deposition in newly formed opening-mode fractures associated with a dextral strike-slip regime. Flow directions of fluids are upward with a strong horizontal component (Gemmell et al., 1988). (3) Large veins hosted in oblique-slip normal faults have been described from the Caylloma vein district in Peru (Echavarria et al., 2006), but these faults are interpreted to have formed in a regional sinistral strike-slip regime. (4) Linked porphyry and epithermal mineralization in the Emperor gold mine, Fiji, are seen as strongly controlled by the northwest-striking Nasivi strike-slip shear zone associated with formation of the Tavua Caldera (Eaton and Setterfield, 1993). (5) For the bonanza-grade orebodies of the Comstock Lode in Nevada, segregation into compartments of higher and lower permeability is hypothesized to be due to extensional step-overs between dextral shear zones (Berger et al., 2003), but Hudson (2003) and Hudson et al. (2009) emphasize the role of normal faulting. (6) Another deposit that has been attributed to strike-slip fault control is Shila Cordillera, Peru (Cassard et al., 2000; Chauvet et al., 2006).

Normal faulting controlled mineralization at Valerdena, Mexico (Hoffman et al., 2000), Midas, Nevada (Leavitt et al., 2003) and Hishikari, Japan (Naito, 1993). At Hishikari there is simultaneous opening of differently oriented vein segments, which may indicate 3-D strain similar to that seen in the Martha Hill deposit. At Cirotan, West Java, Indonesia, formation of veins and mineralization is attributed to a change from dextral strike-slip to normal faulting (Milési et al., 1994).

More complex controls are indicated for other adularia-sericite epithermal deposits. (1) Enhancement of permeability and mineralization in the Cracow goldfield, Australia (Micklethwaite, 2009) has been linked to transient changes from normal to oblique- or strike-slip faulting due to nearby intrusion of dikes and geometrical complexities at fault step-over zones. (2) In the Gosowong epithermal deposit on Halmahera, Indonesia, purely tensional fissure veins are not associated with any regional faults, but are localized on the crest of a dome caused by intrusion of magma (Gemmell, 2007).

Taken together, these global examples indicate that epithermal gold deposits form in a variety of structural settings, not only as simple extensional jogs in a strike-slip regime. Although complex, the dip-slip extensional control recognized at Martha Hill is within the range of situations seen in other deposits.

Regional tectonic controls outside New Zealand

Adularia-sericite epithermal deposits such as that at the Martha Hill mine form on convergent continental margins, but in a large variety of settings (Sillitoe and Hedenquist, 2003; Simmons et al., 2005). These include extensional arc, extensional back-arc during normal subduction as well as during a transition from subduction to rift-related bimodal volcanism, change from subduction margin to transform margin, postcollisional extension due to tectonic collapse and even compression along a transform boundary, or during postcollisional slab break-off. For example, epithermal deposits in northern Nevada are linked to deep fractures associated with the northern Nevada rift (John, 2001; Ponce and Glen, 2002), and Kesler et al. (2004) attributed control of mineralization in the Camagüey district of Cuba to extensional unroofing coupled with thrusting due to the oblique convergence of Cuba with Yucatan. Therefore, variability in the regional tectonic setting of epithermal deposits exhibits a first-order control on their structural complexity, and on the variability in their structural controls from normal to strike-slip faulting.

Regional tectonic controls for Martha Hill mine

There is no direct evidence so far for any major strike-slip faults or thrusts in the Coromandel peninsula (Spörli et al., 2006), and we broadly agree with Sillitoe and Hedenquist (2003) that Hauraki goldfield mineralization formed in a neutral-stress to mildly extensional environment in a continental margin arc. However, it coincided with reorganization of major volcanic arcs from the northwest-southeast–trending Northland arc to the northeast-southwest–trending Colville arc (Brathwaite and Skinner, 1997; Mauk et al., 2011). A southward decrease in age of mineralized veins and differences in vein orientations (Fig. 1), have been directly linked to this migration (Mauk et al., 2011). The question of how the orientations of mineralized veins relate to the overall tectonics of volcanic arcs is complex and largely unresolved by direct observations in active arcs. The simplest scenario is that extension is perpendicular to the arc, forming veins that strike parallel to the arc. This could apply to the northeast strikes of veins in the southern part of the Coromandel goldfield in relation to the northeast-striking Colville arc. However, vein strikes in the north are more varied. Apart from local disturbances, regional causes for this could include stronger coupling in the northern subduction zone with the overlying continental edge plate and therefore some imprint of any oblique subduction, geometric control on fracturing by irregularities in the offshore continental margin or direct interference between the structural trends of the Northland and Colville arcs.

Mineralization in the Martha mine, and probably in a number of other deposits in the area, is characterized by shear-mode faults that change into opening-mode veins, which may indicate a regional increase in horizontal extension. This may be associated with the 0.9-m.y.-long most significant pulse of epithermal mineralization in the Hauraki goldfield (Mauk et al., 2011).

Conclusions

The main events in the upper parts of the Martha Hill mine occurred in the following sequence (Fig. 17), although there is considerable overlap between the early phases: (1) deposition of the Coromandel Group volcanic rocks, (2) initial tectonic fracturing, (3) intrusion of clastic sills and dikes, (4) onset of alteration, (5) main phase of faulting, (6) main phase of veining, (7) erosion and deep oxidation, (8–11) deposition of further volcanic material, including ignimbrite and rhyolite, and formation of present topography.

A complex mesh of faults with relatively small displacements was mostly formed prior to the veins. Dominant movement was normal dip-slip and involved northwest-southeast, north-south, and east-west extension, implying complex 3-D strain. During faulting, north-south extension predated northwest-southeast extension, but the place of east-west extension in the sequence of events is not known. Faults cutting through previously weakened rock commonly showed semiductile behavior. Clastic dikes containing carbonaceous sediments from the country rocks were injected during faulting, reflecting transient high fluid pressures.

Within the northeast-striking mineralized block of the Martha Hill mine, the smaller scale vein stockwork was geometrically complex. It can be considered to be a mesh composed of two arrays, each consisting of orthogonal veins: one with northeast-southwest– and northwest-southeast–striking vein sets, the other with north-south and east-west sets of veins. The northeast-striking Martha and Welcome Lodes eventually became the dominant features both in terms of vein thickness and ore content. Many veins exploited previously established faults, inheriting their anastomosing patterns and other complexities.

Some of the mineralization therefore occurred along faults that changed from initial shear deformation into opening-mode deformation. Such opening of previously sealed fault surfaces must also have operated in other deposits, where

hanging wall and/or footwall faults persist along major veins (e.g., Hudson, 2003; Echavarria et al., 2006; Haworth and Briggs, 2006; Begbie et al., 2007). The opening of faults to facilitate vein formation may have been aided by regional uplift of the kind recognized as a crucial process in deposits elsewhere (e.g., Kesler et al., 2004).

In the stockwork, the sequence of vein formation began with northwest-striking veins and continued through northeast to east-west and north-south strikes. However, during the main vein development, opening oscillated among different directions, with the main northeast-striking veins, Martha and Welcome, capturing a larger portion of the strain increments, either because at some stages of the veining process they were acting as the main connecting "footwall veins" in an upward-diverging pattern, and/or because their controlling fault zones were weaker than those of the minor veins. In addition, the 3-D strain may have been enhanced by the interaction of the northeast-striking fault-vein patterns with an as yet unknown feature that controls the west-northwest–east-southeast trend suggested by us for the location of the gold deposits in the Waihi upflow system (Fig. 2).

The veins and faults in the Waihi upflow system record tectonic controls dominated by northwest-southeast extension and normal dip-slip deformation. Strike-slip faulting is very rare and of only minor importance. This is in accordance with the fact that no major synmineralization strike-slip faulting has yet been rigorously demonstrated in the Hauraki goldfield. Instead, a tectonic framework dominated by extension at the intersection of the northeast trend of the Coromandel arc-Havre Trough-Colville Ridge system and the north-northwest trend of the continental crust-oceanic crust boundary along the peninsula, also highlighted by the Hauraki Rift, contributes additional 3-D strain effects to the local complexities (Spörli et al., 2006).

The following consequences for structural control of epithermal mineral deposits can be derived from our study: as the dominant age relationships between faults and veins in the deposit at Martha Hill mine indicate, some of the veins were formed by a change from shear mode movement on the faults to extensional opening of fractures. Fluid flow was focused into the Martha Hill mine deposit because of extensional opening of a fault network more intensive, complicated and multidirectional than in other mineral deposits of the Hauraki goldfield. Complexity was due to the superposition of local structural northeast and northwest cross-trends with regional tectonic north-south and east-west trends combined with locally concentrated northwest-southeast extension. Thus, structural control in an epithermal mineral deposit can be simultaneously governed by several tectonic causes at different scales. In the case of the deposit at Martha Hill mine, this provided a 3-D extensional environment and a large Au endowment facilitated by the development of lodes with exceptional width and length along strike and dip.

Acknowledgments

Both authors gratefully acknowledge the support of HC by Waihi Gold Mining Company during his M.Sc. work, and the feedback provided by Don McKay, Craig Bosel, and Dean Frederickson. We are indebted to Jeff Mauk for shepherding this manuscript through several versions and making very important suggestions for improving the content. The regular discussion sessions within his Mineral Deposits Group were also of great value. We appreciate Huko Kobe's comments on an earlier version of the manuscript. Louise Cotterall provided sterling assistance with the photos and final preparation of the figures. Mark Simpson helped with getting some of the regional geology figures up to scratch. Helen Cocker commented on the table presenting the sequence of events. Byron Berger, David John, Stephen Box, and an anonymous reviewer made numerous important suggestions clarifying our arguments and helped to reduce the amount of structural geology jargon. We thank Newmont Waihi Gold Limited, the present operators of the mine, for giving permission to publish.

REFERENCES

Adams, C.J., and Maas, R., 2004, Age/isotopic characteristics of the Waipapa Group in Northland and Auckland, New Zealand, and implications for the status of the Waipapa terrane: New Zealand Journal of Geology and Geophysics, v. 47, p. 173–178.

Aleksandrowski, P., 1985, Graphical determination of principal stress directions for slickenside lineation populations: Journal of Structural Geology, v. 7, p. 73–82.

Anderson, E.M., 1951, The dynamics of faulting and dyke formation, with application to Britain, 2nd edition: Edinburgh, Oliver and Boyd, 206 p.

Andrews, B.J., 2003, The phreatomagmatic formation of polyphase clastic dikes, Moeraki Peninsula, South Island, New Zealand [abs.]: Geological Society of America Annual Meeting Abstracts with Programs, v. 35, p. 320.

Angelier, J., 1984, Tectonic analysis of fault slip data sets: Journal of Geophysical Research, B7, Solid Earth and Planets, v. 89, p. 5835–5848.

Beach, A., 1977, Vein arrays, hydraulic fracture and pressure solution features in deformed Flysch sequences, southwest England: Tectonophysics, v. 40, p. 201–225.

Begbie, M.J., Spörli, K.B., and Mauk, J.L., 2007, Structural evolution of the Golden Cross Epithermal Au-Ag deposit, New Zealand: Economic Geology, v. 102, p. 873–892.

Berger, B.R., Tingley, J.V., and Drew, L.J., 2003, Structural localization and origin of compartmentalized fluid flow, Comstock Lode, Virginia City, Nevada: Economic Geology, v. 98, p. 387–408.

Brathwaite, R.L., and Christie, A.B., 1996, Geology of the Waihi area, scale 1:50,000: Institute of Geological and Nuclear Sciences, Geological Map 21, 1 sheet + 64 p.

Brathwaite, R.L., and Faure, K., 2002, The Waihi gold-silver-base metal sulfide-quartz vein system, New Zealand: Temperature and salinity controls on electrum and sulfide deposition: Economic Geology, v. 97, p. 269–290.

Brathwaite, R.L., and Mc Kay, D.F., 1989, Geology and exploration of the Martha Hill gold-silver deposit, Waihi, *in* Kear, D., ed., Mineral deposits of New Zealand, Australasian Institute of Mining and Metallurgy, Monograph 13, p. 83–88.

Brathwaite, R.L., and Skinner, D.N.B., 1997, The Coromandel epithermal gold-silver province: A result of collision of the Northland and Colville volcanic arcs in northern New Zealand: 1997 New Zealand Minerals and Mining Conference, Publicity Unit, Crown Minerals, Ministry of Commerce, Wellington, Proceedings, p. 111–117.

Brathwaite, R.L., McKay, D.F., and Henderson, S., 1986, The Martha Hill gold-silver deposit, Waihi, *in* Braithwaite, R.L., Browne, P.R.L., and Roberts, P.J., eds., Symposium 5, Volcanism, hydrothermal systems and related mineralisation, International Volcanological Congress, Auckland, New Zealand, Proceedings, p. 19–23.

Brathwaite, R.L., Christie, A. B., and Skinner, D.N.B., 1989, The Hauraki Goldfield- regional setting, mineralisation, and recent exploration, *in* Kear, D., ed., Mineral deposits of New Zealand: Australasian Institute of Mining and Metallurgy, Monograph 13, p. 45–56.

Brathwaite, R.L., Cargill, H.J., Christie, A.B., and Swain, A., 2001, Lithological and spatial controls on the distribution of quartz veins in andesite- and rhyolite-hosted epithermal Au-Ag deposits of the Hauraki goldfield, New Zealand: Mineralium Deposita, v. 36, p. 1–12.

Brathwaite, R.L., Torckler, L.K, and Jones, P.K., 2006, The Martha Hill epithermal Au-Ag deposit, Waihi—Geology and Mining History, *in* Christie, A.B. and Brathwaite, R.L., eds., Geology and Exploration of New Zealand

Mineral Deposits: Australasian Institute of Mining and Metallurgy Monograph, v. 25, p. 171–178.
Briggs, R.M., and Krippner, S.J.P., 2006, The control by caldera structures on epithermal Au-Ag mineralisation and hydrothermal alteration at Kapowai, central Coromandel volcanic zone, *in* Christie, A.B., and Brathwaite, R.L., eds., Geology and Exploration of New Zealand Mineral Deposits: Australasian Institute of Mining and Metallurgy Monograph, v. 25, p. 101–107.
Browne, P.R.L., and Lawless, J.V., 2001, Characteristics of hydrothermal eruptions, with examples from New Zealand and elsewhere: Earth-Science Reviews, v. 52, p. 299–331.
Cargill, H., 1994, Aspects of the structural geology of the Martha Hill epithermal Au-Ag deposit, New Zealand: Unpublished M.Sc. thesis, New Zealand, University of Auckland, 96 p.
Cassard, D., Chauvet, A., Bailly, L., Tajada, F.L., Vargas, J.R., Marcoux, E., and Lerouge, C., 2000, Structural control and K/Ar dating of the Au-Ag epithermal veins in the Shila Cordillera, southern Peru: Comptes Rendus Academie des Sciences, Serie II, Sciences de la Terre et des Planetes, v. 330, p. 23–30.
Chauvet, A., Bailly, L., André, A., Monié, P., Cassard, D., Tajada, F.L., Vargas, J.R., and Tuduri, J., 2006, Internal vein texture and vein evolution of the epithermal Shila-Paula district, southern Peru: Mineralium Deposita, v. 41, p. 387–410.
Christie, A.B., Brathwaite., R.L., Mauk, J.L., and Simpson, M.P., 2006, Hauraki goldfield—regional exploration databases and prospectivity studies, *in* Christie, A.B., and Brathwaite, R.L., eds., Geology and Exploration of New Zealand Mineral Deposits: Australasian Institute of Mining and Metallurgy Monograph, v. 25, p. 73–84.
Christie, A.B., Simpson, M.P., Brathwaite, R.L., and Mauk, J.L., 2007, Epithermal Au-Ag and related deposits of the Hauraki goldfield, Coromandel volcanic zone, New Zealand: Economic Geology, v. 102, p. 785–816.
Cosgrove, J.W., 2001, Hydraulic fracturing during the formation and deformation of a basin: A factor in dewatering of low-permeability sediments: American Association of Petroleum Geologists Bulletin, v. 85, p. 737–748.
Davies, A.G.S., Cooke, D.R., Gemmell, J.B., and Simpson, K.A., 2008a, Diatreme Breccias at the Kelian Gold Mine, Kalimantan, Indonesia: Precursors to epithermal gold mineralization: Economic Geology v. 103, p. 689–716.
Davies, A.G.S., Cooke, D.R., Gemmell, J.B., Van Leeuwen, T., Cesare, P., and Hartshorn, G., 2008b, Hydrothermal breccias and veins at the Kelian gold mine, Kalimantan, Indonesia: Genesis of a large epithermal gold deposit: Economic Geology, v. 103, p. 717–757.
DeGraff, J.M., and Aydin, A., 1987, Surface morphology of columnar joints and its significance to mechanics and direction of joint growth: Geological Society of America Bulletin, v. 99, p. 605–617.
Dix, G.R., and Nelson, C.S., 2004, The role of tectonism in sequence development and facies distribution of upper Oligocene cool water carbonates: Coromandel peninsula, New Zealand: Sedimentology, v. 51, p. 231–251.
Dong, G., Gregg, M., and Subhash, J., 1995, Quartz textures in epithermal veins, Queensland—classification, origin, and implications: Economic Geology, v. 90, p. 1841–1856.
Eaton, P.C., and Setterfield, T.N., 1993, The relationship between epithermal and porphyry hydrothermal systems within the Tavua Caldera, Fiji: Economic Geology, v. 88, p. 1053–1083.
Echavarria, L., Nelson, E., Humphrey, J., Chavez, J., Leopoldo, E., and Iriondo, A., 2006, Geologic evolution of the Caylloma epithermal vein district, southern Peru: Economic Geology, v. 101, p. 843–863.
Egan, M.J., and Alshley, P.M., 1992, The Devils Chimney breccia pipe, Dyamberin area, northeastern New South Wales: Australian Journal of Earth Sciences, v. 39, p. 239–247.
Etchecopar, A., Vasseur, G., and Daignieres, M., 1981, An inverse problem in microtectonics for the determination of stress tensors from fault striation analysis: Journal of Structural Geology, v. 3, p. 51–65.
Ford, D.C., and Williams, P.W., 2007, Karst hydrogeology and geomorphology: Chichester, UK, John Wiley & Sons, 562 p.
Gadsby, M.R., and Spörli, K.B., 1989, Structural background to Hauraki goldfield mineralisation: A review, 2nd Geothermal workshop, University of Auckland, Geothermal Institute, Proceedings, v. II, p. 149–154.
Gadsby, M. R., Spörli, K.B., and Clarke, D.S., 1990, Structural elements in epithermal gold deposits of the Coromandel peninsula, New Zealand Australasian Institute of Mining and Metallurgy Conference, Rotorua, New Zealand, 1990, Proceedings, p. 145–151.
Gemmell, J. B., 2007, Hydrothermal alteration associated with the Gosowong epithermal Au-Ag deposit, Halmahera, Indonesia: Mineralogy, geochemistry and exploration implications: Economic Geology, v. 102, p. 893–922.
Gemmell, J.B., Simmons, S.F., and Zantop, H., 1988, The Santo Niño silver-lead-zinc vein, Fresnillo district, Zacatecas, Mexico: Part I, structure, vein stratigraphy, and mineralogy: Economic Geology, v. 83, p. 1597–1618.
Grossenbacher, K.A., and McDuffie, S.M., 1995, Conductive cooling of lava: Columnar joint diameter and striae width as function of cooling rate and thermal gradient: Journal of Volcanology and Geothermal Research, v. 69, p. 95–103.
Hancock, P.L., 1985, Brittle microtectonics: Principles and practice: Journal of Structural Geology, v. 7, p. 437–457.
Harding, T.P., 1985, Seismic characteristics and identification of negative flower structures, positive flower structures, and positive structural inversion: American Association of Petroleum Geologists Bulletin, v. 69, p. 582–600.
Haworth, A.V., and Briggs, R.M., 2006, Epithermal Au-Ag mineralisation in the lower Waitekauri valley, Hauraki goldfield, *in* Christie, A.B., and Brathwaite, R.L., eds., Geology and Exploration of New Zealand Mineral Deposits: Australasian Institute of Mining and Metallurgy Monograph, v. 25, p. 157–162.
Hayward, B.W., Black, P.M., Smith, I.E.M., Ballance, P.F., Itaya, T., Doi, M., Takagi, M., Bergman, S., Adams, C.J., Herzer, R.H., and Robertson, D.J., 2001, K-Ar ages of early Miocene arc-type volcanoes in northern New Zealand: New Zealand Journal of Geology and Geophysics, v. 44, p. 285–311.
Hayward, B.W., Grenfell, H. R., Mauk, J. L, and Moore, P.R., 2006, The west-flowing "Clevedon River," Auckland: Geological Society of New Zealand Newsletter, v. 141, p. 24–29.
Hobbins, J. M, 2009, Near mine exploration challenges and opportunities at Waihi, New Zealand: Annual Conference of the New Zealand Branch of the AusIMM, 2009, Queenstown, New Zealand. Proceedings, p. 201–210.
Hochstein, M.P., and Ballance, P.F., 1993, Hauraki Rift: A young active, intracontinental rift in a back-arc setting, *in* Ballance, P.F., ed., Sedimentary Basins of the World v. 2, South Pacific Sedimentary Basins, Amsterdam, Elsevier, p. 295–305.
Hoffman, E., Tremblay, A., and Pinet, N., 2000, Structural analysis of mineralization and late faulting at the Velardena mine, central Mexico [abs.]: Geological Society of America, Northeastern Section, Abstracts with Programs, v. 32, p. 25.
Hudson, D.M., 2003, Epithermal alteration and mineralization in the Comstock District, Nevada: Economic Geology, v. 98, p. 367–385.
Hudson, D.M., Castor, S.B., Garside, L.J., and Henry, C.D., 2009, Geologic map of the Virginia City Quadrangle, Washoe, Storey and Lyon Counties and Carson City, Nevada: Nevada Bureau of Mines and Geology Map 165, (http://www.nbmg.unr.edu/dox/m165.pdf), scale 1:24,000.
Jébrak, M., 1997, Hydrothermal breccias in vein-type ore deposits: A review of mechanisms, morphology and size distribution: Ore Geology Reviews, v. 12, p. 111–134.
John, D.A., 2001, Miocene and early Pliocene epithermal gold-silver deposits in the northern Great Basin, western United States: Characteristics, distribution, and relationship to magmatism: Economic Geology, v. 96, p. 1827–1853.
Katternhorn, S.A., and Pollard, D.D., 2001, Integrating 3-D seismic data, field analogs, and mechanical models in the analysis of segmented normal faults in the Wytch farm oil field, southern England, United Kingdom: American Association of Petroleum Geologists Bulletin, v. 85, p. 1183–1210.
Kesler, S.E., Hall, C.M., Russell, N., Piñero, E., Sánchez, R.C., Pérez, M.R., and Moreira, J., 2004, Age of the Camagüey gold-silver district, Cuba: Tectonic evolution and preservation of epithermal mineralization in volcanic arcs: Economic Geology, v. 99, p. 869–886.
King, P.B., 2000, Tectonic reconstruction of New Zealand: 40 Ma to present: New Zealand Journal of Geology and Geophysics, v. 43, p. 611–638.
Krantz, R.W., 1988, Multiple fault sets and three dimensional strain: Theory and application: Journal of Structural Geology, v. 10, p. 225–237.
Leavitt, E., Spell, T.L., Wallace, A.R., Goldstrand, P., and Arehart, G.B., 2003, Volcano-tectonic setting of the Midas epithermal deposit, Elko County, Nevada [abs.]: Geological Society of America Annual Meeting, Abstracts with Programs, v. 35, p. 61.
Mansfield, C., and Cartwright, J. 2001, Fault growth by linkage; observations and implications from analogue models: Journal of Structural Geology, v. 23, p. 745–763.
Martin, S.B., and Mauk, J.L, 2006, Vein relationships and textures at Martha mine, Waihi: New Zealand Branch of the AusIMM Annual Conference, Proceedings, p. 223–232.

Mauk, J.L., and Hall, C.M., 2004, 40Ar/39Ar ages of adularia from Golden Cross, Neavesville, and Komata epithermal deposits, Hauraki goldfield, New Zealand: New Zealand Journal of Geology and Geophysics, v. 47, p. 227–231.

Mauk, J.L., Hall, C.M., Chesley J.T., and Barra, F., 2011, Punctuated evolution of a large epithermal province: The Hauraki goldfield, New Zealand: Economic Geology, v. 106, p. 921–943.

Micklethwaite, S., 2009, Mechanisms of faulting and permeability enhancement during epithermal mineralisation: Cracow goldfield, Australia: Journal of Structural Geology, v. 31, p. 288–300.

Milési, J.P., Marcoux, E., Neehlig, P., Sunarya, Y., Sukandar, A., and Felenc, J., 1994, Cirotan, West Java, Indonesia: A 1.7 Ma hybrid epithermal Au-Ag-Sn-W deposit: Economic Geology, v. 89, p. 227–245.

Mortimer, N., Herzer, R.H., Gans, P.B., Laporte-Magoni, C., Calvert, A.T., and Bosch, D., 2007, Oligocene-Miocene tectonic evolution of the South Fiji Basin and Northland Plateau, SW Pacific Ocean: Evidence from petrology and dating of dredged rocks: Marine Geology, v. 237, p. 1–24.

Mortimer, N., Gans, P.B., Palin, J.M., Meffre, S., Herzer, R.H., and Skinner, D.N.B., 2009, Location and migration of Miocene-Quaternary volcanic arcs in the SW Pacific region: Journal of Volcanology and Geothermal Research, v. 190, p. 1–10.

Munson, P.J., Munson, C.A., and Pond, E.C., 1995, Paloeliquefation evidence for a strong Holocene earthquake in south-central Indiana: Geology, v. 23, p. 325–328.

Naito, K., 1993, Occurrences of quartz veins in the Hishikari gold deposits, southern Kyushu, Japan: Resource Geology, Special Issue 14, p. 37–46.

Nortje, G.S., Rowland, J.V., Spörli, K.B., Blenkinsop, T.G., and Rabone, S.D.C., 2006, Vein deflections and thickness variations of epithermal quartz veins as indicators of fracture coalescence: Journal of Structural Geology, v. 28, p. 1396–1405.

Panther, C.A., Mauk, J.L., and Arehart, G,B., 1995, A petrographic and oxygen isotope study of banded epithermal veins from the Martha Hill Au-Ag mine, Waihi, New Zealand, *in* Mauk, J.L., and St George, J.D., eds., Proceedings of the 1995 PACRIM Congress: The Australasian Institute of Mining and Metallurgy, v. 9/95, p. 447–452.

Passchier, C.W., and Trouw, R.A.J., 1998, Microtectonics: Berlin, Springer Verlag, 289 p.

Pollard, D.D., and Aydin, A., 1988, Progress in understanding jointing over the past century: Geological Society of America Bulletin, v. 100, p. 1181–1204.

Ponce, D.A., and Glen, J.M.G., 2002, Relationship of epithermal gold deposits to large scale fractures in northern Nevada: Economic Geology, v. 97, p. 3–9.

Raymond, L.A., 1984, Classification of melanges, *in* Raymond, L.A., ed., Melanges, their nature, origin and significance: Geological Society of America Special Paper, v. 198, p. 7–20.

Rowland, J.V., and Sibson, R.H., 2004, Structural controls on hydrothermal flow in a segmented rift system, Taupo Volcanic Zone, New Zealand: Geofluids v. 4, p. 259–283.

Rowland, J. V., Baker, E., Ebinger, C.J., Keir, D., Kidane, T., Biggs, J., Hayward, N., and Wright, T.J., 2007, Fault growth at a nascent slow-spreading ridge: 2005 Dabbahu rifting episode, Afar: Geophysical Journal International, v. 171. p. 1226–1246.

Schaefer, C.J., and Kattenhorn, S.A., 2004, Characterization and evolution of fractures in low-volume pahoehoe lava flows, eastern Snake River Plain, Idaho: Geological Society of America Bulletin, v. 116, p. 322–336.

Shan, Y., Tian, Y., and Wenjiao Xia, W., 2009, Incorporating imaginary faults in graphical stress methods: Journal of Structural Geology, v. 31, p. 366–368.

Sibson, R.H., 1987, Earthquake rupturing as a mineralising agent in hydrothermal systems: Geology, v. 15, p. 701–704.

Sibson, R.H., 1996, Structural permeability of fluid driven fault-fracture meshes: Journal of Structural Geology, v. 18, p. 1031–1042

Sillitoe, R.H., and Hedenquist, J.W., 2003, Linkages between volcanotectonic settings, ore-fluid compositions, and epithermal precious metal deposits: Society of Economic Geologists Special Publications, no. 10, p. 315–343.

Simmons, S.F., White, N.C., and John, D.A., 2005, Geological characteristics of epithermal precious and base metal deposits: Economic Geology 100th Anniversary Volume, p. 485–522.

Simpson, M.P., and Mauk. J.L., 2007, The Favona epithermal gold-silver deposit, Waihi, New Zealand: Economic Geology, v. 102, p. 817–839.

Skinner, D.N.B., 1976, Northern Coromandel: Geological Map of New Zealand: Department of Scientific and Industrial Research, Wellington, Sheet N40 and part sheet N35, N36 and N39, 1:36,360.

Skinner, D.N.B., 1986, Neogene volcanism of the Hauraki volcanic region, *in* Smith, I.E.M., ed., Late Cenozoic volcanism in New Zealand: Royal Society of New Zealand Bulletin, v. 23, p. 21–47.

Smith, N., Cassidy, J., Locke, C.A., Mauk, J.L., and Christie, A.B., 2006, The role of regional-scale faults in controlling the development of a trap-door caldera, Coromandel peninsula, New Zealand: Journal of Volcanology and Geothermal Research, v. 149, p. 312–328.

Soliva, R., and Schultz, R.A., 2008, Distributed and localized faulting in extensional settings: Insight from the North Ethiopian Rift—Afar transition area: Tectonics, v. 27, TC2003.

Spörli, K.B., 1987, Development of the New Zealand microcontinent, *in* Monger, J.W.H., and Francheteau, J., eds., Orogenic belts and evolution of the Pacific ocean basin: American Geophysical Union, Geodynamics Series, v. 19, p. 115–132.

Spörli, K.B., Begbie, M.J., Irwin, M.R., and Rowland, J.V., 2006, Structural processes and tectonic controls in epithermal Au-Ag deposits of the Hauraki goldfield, New Zealand, *in* Christie, A.B., and Brathwaite, R.L., eds., Geology and exploration of New Zealand mineral deposits, Australasian Institute of Mining and Metallurgy Monograph, v. 25, p. 85–94.

Stevens, M.R., and Boswell, G.B., 2006, Review of exploration and geology of the Karangahake Au-Ag deposit, Hauraki goldfield, *in* Christie, A.B., and Brathwaite, R.L., eds., Geology and exploration of New Zealand mineral deposits, Australasian Institute of Mining and Metallurgy Monograph, v. 25, p. 163–170.

Sylvester, A.G., 1988, Strike-slip faults: Geological Society of America Bulletin, v. 100, p. 1666–1703.

Torckler, L.K., Mc Kay, D., and Hobbins, J., 2006, Geology and exploration of the Favona Au-Ag deposit, Waihi, Hauraki goldfield, *in* Christie, A.B., and Brathwaite, R.L., eds., Geology and Exploration of New Zealand Mineral Deposits, Australasian Institute of Mining and Metallurgy Monograph, v. 25, p. 179–184.

Townend, J., and Zoback, M.D., 2005, Stress, strain, and mountain building in central Japan: Journal of Geophysical Research, v. 111, p. B03411, doi: 10.1029/2005JB003759.

Van Leeuwen, T.M., Leach, T., Hawke, A.A., and Hawke, M.M., 1990, The Kelian disseminated gold deposit, East Kalimantan, Indonesia: Journal of Geochemical Exploration, v. 35, p. 1–61.

Wellman, H.W., 1954, Stress patterns controlling lode formation and faulting at Waihi mine and notes on the stress patterns in the northwestern part of the North Island: New Zealand Journal of Science and Technology, v. 36B, p. 201–206.

Wilcox, R.E., Harding, T, P., and Seely, D.R., 1973, Basic wrench tectonics: American Association of Petroleum Geologists Bulletin, v. 57, p. 74–96.

Willis, G. F., and Tosdal, R.M., 1992, Formation of gold veins and breccias during dextral strike-slip faulting in the Mesquite mining district, southeastern California: Economic Geology, v. 87, p. 2002–2022.

Wojtal, S.F., 2001, The nature and origin of asymmetric arrays of shear surfaces in fault zones, *in* Holdsworth, R.E., Strachan, R.A., Macloughlin, J.F., and Knipe, R.J., eds., The nature and tectonic significance of fault zone weakening: Geological Society of London Special Publication, v. 186, p. 171–193.